

NOVEL RADIATION GRAFTED MEMBRANES BASED ON FLUORINATED POLYMERS
FOR PROTON EXCHANGE MEMBRANE FUEL CELL

by

SAHL SADEGHI

Submitted to the Graduate School of Engineering and Natural Sciences
in partial fulfillment of the requirements for the degree of Master of Science

Sabanci University

August 2016

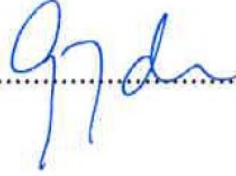
NOVEL RADIATION GRAFTED MEMBRANES BASED ON FLUORINATED POLYMERS
FOR PROTON EXCHANGE MEMBRANE FUEL CELL

APPROVED BY:

Assoc. Prof. Dr. Selmiye Alkan Gürsel
(Thesis Supervisor)


.....

Assoc. Prof. Dr. Gozde Ince


.....

Asst. Prof. Dr. Oktay Demircan


.....

DATE OF APPROVAL: 9 Aug 2016

© Sahl Sadeghi 2016

All Rights Reserved

NOVEL RADIATION GRAFTED MEMBRANES BASED ON FLUORINATED POLYMERS FOR PROTON EXCHANGE MEMBRANE FUEL CELL

SAHL SADEGHI

MAT, M.Sc. Thesis, 2016

Thesis Supervisor: Assoc. Prof. Selmiye Alkan Gürsel

ABSTRACT

In the first part of this thesis a facile method for preparing poly(vinylidene fluoride) (PVDF)-*g*-poly(styrene sulfonate acid) (PSSA) membranes by radiation induced graft polymerization is reported. Sodium styrene sulfonate (SSS) monomer has been used for the grafting of SSS from PVDF powder in aqueous dimethyl sulfoxide (DMSO) solution, and it precipitated after synthesis. Later on, the resultant PVDF-*g*-PSSS graft copolymer membranes were prepared by means of vapor induced phase separation (VIPS) technique at 60% relative humidity (RH), and dried under vacuum at high temperature to achieve PVDF-*g*-PSSA proton conducting nano-porous membranes. It was found that these membranes exhibit encouraging results in terms of higher conductivity and better mechanical properties compared to Nafion[®] NR-211.

In the second part of thesis, the effect of divinylbenzene (DVB) as a cross-linker on the graft polymerization of 4-vinylpyridine (4-VP) from poly(ethylene-*co*-tetrafluoroethylene) (ETFE) films was studied. The resulted films were doped with phosphoric acid (PA), and examined for mechanical properties and fuel cell performance. The cross-linked membrane obtained from grafting a mixture of 4-VP with 1% DVB improved the polymerization kinetics, and resulted in 50% graft level (GL). The resulted membrane additionally exhibited proton conductivity as high as 75 mS/cm at 50% relative humidity and 120 °C, besides doubling the power output of fuel cell comparing to a non-cross-linked membrane.

PROTON DEĞİŞİM MEMBRANLI YAKIT HÜCRESİ İÇİN FLORÜRLÜ POLİMER ESASLI RADYASYONLA AŞILANMIŞ ÖZGÜN MEMBRANLAR

SAHL SADEGHI

MAT, M.Sc. Tezi, 2016

Tez danışmanı: Doç. Dr. Selmiye Alkan Gürsel

ÖZET

Tezin ilk bölümünde polistiren sülfonik asit esaslı polivinilidin florür (PVDF-g-PSSA) membranlarının radyasyonla aşılama polimerizasyonu ile hazırlanması açıklanmıştır. Sodyum stiren sülfonat monomeri toz haldeki PVDF ile dimetil sülfoksit ortamında aşılama sırasında kullanılmış ve sentez sonrası çökmesi sağlanmıştır. Daha sonra, PVDF-g-PSSA kopolimer membranları buhar esaslı faz dönüşüm tekniği ile %60 bağıl nemde sentezlenmiş, sıcak vakum ortamında kurutularak proton değişimli nano-gözenekli yapı elde edilmiştir. Üretilen bu membranların ticari Nafion® NR-211 membranına kıyasla yüksek iletkenlik ve iyileştirilmiş mekanik özellikleri açısından ümit verici özellikler sergilediği gözlemlenmiştir.

Tezin ikinci bölümünde, divinilbenzen (DVB) çapraz bağlayıcısının polietilen tetrafloroetilen (ETFE) filmleri üzerinde 4-vinilpiridin (4-VP) ile polimerleşerek aşılama üzerinde durulmuştur. Aşılama filmler fosforik asit ile katkılılandırdıktan sonra mekanik özellikleri ve yakıt hücresi performansı bakımından karakterize edilmiştir. 4-VP ve %1 DVB içeren aşılama çözeltisiyle üretilmiş çapraz bağlı membranlar, ileri polimerizasyon kinetikleriyle %50 aşılama derecesi sağlamıştır. Üretilen çapraz bağlı membranların 120°C sıcaklığında %50 bağıl nemde 75 mS/cm gibi yüksek iletkenlik göstermesinin yanı sıra çapraz bağlı olmayan membranlara göre iki kat daha fazla güç yoğunluğu sağlamıştır.

“Education is not preparation for life; education is life itself.”

- John Dewey

ACKNOWLEDGEMENTS

I would like to extend my sincerest appreciation and thanks to my supervisor professor Dr. Selmiye Alkan Gursel. I would like to thank you for encouraging my research and for allowing me to grow as a research scientist. I would also like to thank Prof. Dr. Gozde Ince and Prof. Dr. Oktay Demircan for serving as my committee members, and for your brilliant comments and suggestions. I would also like to take the chance to appreciate my instructors in faculty of engineering and natural science of Sabanci university who patiently helped me to extend my knowledge in my field of research. My special thanks go to my colleagues, friends and researchers at SUNUM facility, especially my mentors Dr. Enver Guler, Dr. Veera Sadhu, Dr. Lale I. Sanli who supported me as friends.

TABLE OF CONTENT

| | |
|--|------|
| ABSTRACT..... | iv |
| ÖZET | v |
| ACKNOWLEDGEMENTS..... | vii |
| TABLE OF CONTENT..... | viii |
| LIST OF FIGURES | xi |
| LIST OF TABLES..... | xiv |
| LIST OF EQUATION | xv |
| ABBREVIATIONS AND SYMBOLS..... | xvi |
| 1. INTRODUCTION | 1 |
| 1.1. History of fuel cell..... | 1 |
| 1.2. Types of fuel cells..... | 2 |
| 1.2.1. Low temperature fuel cells..... | 3 |
| 1.2.2. Intermediate temperature fuel cells..... | 5 |
| 1.2.3. High temperature fuel cells..... | 6 |
| 1.3. Governing principles for proton exchange fuel cell..... | 7 |
| 1.4. Proton exchange membranes | 14 |
| 1.4.1. Fluorinated proton exchange membranes | 16 |
| 1.4.2. Sulfonic polymers and processes | 19 |
| 1.4.3. Radiation induced graft polymerization..... | 20 |
| 2. NANO-STRUCTURED POLY(VINYDENE FLUORIDE) GRAFT POLYSTYRENE SULFONIC ACID FOR PROTON EXCHANGE MEMBRANE | 23 |
| 2.1. Introduction..... | 24 |
| 2.2. Experimental..... | 26 |

| | |
|---|-----------|
| 2.2.1. Material..... | 26 |
| 2.2.2. Radiation induced graft copolymerization..... | 26 |
| 2.2.3. Membrane preparation..... | 27 |
| 2.2.4. Characterization of membranes..... | 27 |
| 2.3. Results and discussion..... | 28 |
| 2.3.1. Graft level..... | 30 |
| 2.3.2. Water up-take..... | 31 |
| 2.3.3. Proton conductivity..... | 32 |
| 2.3.4. Thermogravimetric analysis..... | 34 |
| 2.3.5. Mechanical properties..... | 34 |
| 2.3.6. Fuel Cell performance..... | 35 |
| 2.4. Conclusions..... | 36 |
| 3. CROSS-LINKED PROTON EXCHANGE MEMBRANES BY RADIATION INDUCED GRAFTING OF 4-VINYLPYRIDINE AND DIVINYLBENZENE FROM POLY(ETHYLENE- CO-TETRAFLUOROETHYLENE) FILMS..... | 37 |
| 3.1. Introduction..... | 38 |
| 3.2. Experimental..... | 40 |
| 3.2.1. Materials..... | 40 |
| 3.2.2. Membrane preparation..... | 41 |
| 3.2.3. Characterization of membranes..... | 41 |
| 3.3. Results and discussion..... | 42 |
| 3.3.1. The effect of reaction time on graft level..... | 42 |
| 3.3.2. The Effect of DVB concentration on graft level..... | 43 |
| 3.3.3. The effect of DVB on phosphoric acid up-take..... | 44 |
| 3.3.4. The effect of DVB on phosphoric acid loss..... | 45 |
| 3.3.5. The effect of DVB on mechanical properties of membranes..... | 47 |

| | |
|--|----|
| 3.3.6. Ionic conductivity of grafted membranes | 47 |
| 3.3.7. Fuel cell performance of ETFE-g-PVP membranes | 48 |
| 3.4. Conclusion | 49 |
| REFERENCES | 51 |

LIST OF FIGURES

| | |
|--|----|
| Figure 1. 1. Schematic of Sir William Grove fuel cell 1839 [6]. | 1 |
| Figure 1. 2. Classification of current commercial fuel cell technologies [8]. | 2 |
| Figure 1. 3. Comparison of proton exchange fuel cell (PEFC) and anion exchange membrane fuel cell (AEMFC) [18]. | 4 |
| Figure 1. 4. Materials and related issues for SOFC [46]. | 7 |
| Figure 1. 5. The effect of temperature vs. cell voltage $E^{\circ}(v)$ for hydrogen and methane as fuel [73]. | 11 |
| Figure 1. 6. Typical performance of a hydrogen fuel cell and the effect of common overpotentials [73]. | 13 |
| Figure 1. 7. Semiempirical potential energy for proton transfer across hydrogen bindings of symmetrical conformations of the type R-O-H...O-R for different oxygen distances Q and full stabilization of the surrounding [76]. | 14 |
| Figure 1. 8. Scheme of the hypothetical mechanism, in which a Grotthuss-type mechanism is occurred by a short-distance transportation of hydronium ions [82]. | 15 |
| Figure 1. 9. Proton conductivity system of phosphoric acid-doped PBI (a) phosphoric acid –water hydrogen ion transfer; (b) benzimidazole – phosphoric acid proton transfer; (c) hopping between phosphoric acid [27]. | 16 |
| Figure 1. 10. A) Nafion® B) Aquivion® C) 3M structures [92]. | 17 |
| Figure 1. 11. Different synthesis pathways for perfluoro(alkyl vinyl ether) with sulfonyl acid fluoride, above) DuPont method for Nafion®, below) Solvay method for Aquivion [93]. | 18 |
| Figure 1. 12. 3M method for synthesizing perfluoro(alkylvinyl ether) with sulfonyl acid fluoride monomer [95]. | 18 |
| Figure 1. 13. Schematic of sulfonation of poly(ether ether ketone) (PEEK) by concentrated sulfuric acid [106]. | 19 |
| Figure 1. 14. Synthetic methods for preparing comb-like polymers: (a) “Grafting-onto” is the grafting of functional side chains to a polymeric backbone with active groups. (b) “Grafting-through” comprises of the polymerization process of functionalized monomers. (c) “Grafting-from” is the grafting of co-polymerization of vinyl monomers on a polymeric backbone with active sites [114]. | 20 |
| Figure 1. 15. Plausible mechanism of preparation of phosphoric acid doped poly(4-VP) grafted ETFE | |

| | |
|--|----|
| membrane [133]. | 21 |
| Figure 2. 1. ¹ H-NMR result of PVDF-g-PSSS, “a” peaks belong to PVDF, and “b” and “c” peaks belong to SSS. | 30 |
| Figure 2. 2. Graft level of PVDF-g-PSSS with respect to reaction time. | 31 |
| Figure 2. 3. The relation between graft level and water up-take of membranes prepared by VIPS method. | 32 |
| Figure 2. 4. Proton conductivity of the membranes prepared by tape casting and mold casting. | 33 |
| Figure 2. 5. Scanning electron microscopy imaging of sub-micron structure of PVDF-g-PSSS membrane with 35% graft level. | 33 |
| Figure 2. 6. Thermogravimetric analysis of PVDF-g-PSSA compared to pristine PVDF, PVDF-g-PSSS and Nafion® NR-211. | 34 |
| Figure 2. 7. The universal tensile stress results of fully humidified PVDF-g-PSSA membrane with different graft levels. | 35 |
| Figure 2. 8. Current-voltage and current-power of fuel cell performance of 35% grafted PVDF-g-PSSA at 60°C and 80%RH vs. Nafion® NR-211 at 80°C and 60%RH. | 36 |
| Figure 3. 1. Mechanism of preparation of cross-linked phosphoric acid doped poly(4VP) grafted ETFE membrane. | 40 |
| Figure 3. 2. The graft level of ETFE-g-PVP films with 0%DVB and 1%DVB at 60°C, 50 kGy and varying reaction time. | 43 |
| Figure 3. 3. The effect of DVB concentration on graft level of 50 kGy ETFE films at 60°C and 4 hours grafting time. | 43 |
| Figure 3. 4. The effect of DVB concentration on the phosphoric acid up-take during doping process. | 44 |
| Figure 3. 5. Scanning electron microscope image of grafted ETFE films: left) 0%DVB grafted film right) 1%DVB grafted film. | 45 |
| Figure 3. 6. The effect of DVB on acid up-take and acid loss of grafted membranes with the same initial conditions. | 46 |
| Figure 3. 7. The effect of cross-linking on contact angle of acid doped membranes: left) 0% DVB | |

| | |
|--|----|
| mebrane, right) 1% DVB membrane..... | 46 |
| Figure 3. 8. The tensile test results for acid doped membranes with 0%, 1% and 2% DVB content. | 47 |
| Figure 3. 9. The proton conductivity of ETFE-g-PVP membranes at different relative humidity and temperature..... | 48 |
| Figure 3. 10. Fuel cell performance of ETFE-g-PVP at 50%RH, 1atm and different temperatures..... | 49 |

LIST OF TABLES

| | |
|--|----|
| Table 1. 1. Theoretical and actual efficiencies of different commercial fuel cells and their operating temperatures [8]..... | 3 |
| Table 1. 2. The effect of operating temperature of hydrogen fuel cell on the cell voltage and maximum efficiency[72]. | 11 |
| Table 2. 1. The effect of water content in the polymerization solution to graft level. | 30 |

LIST OF EQUATION

| | |
|---------------------|----|
| Equation 1.1 | 3 |
| Equation 1.2 | 7 |
| Equation 1.3 | 7 |
| Equation 1.4 | 7 |
| Equation 1.5 | 9 |
| Equation 1.6 | 10 |
| Equation 1.7 | 10 |
| Equation 1.8 | 10 |
| Equation 1.9 | 12 |
| Equation 1.10 | 12 |
| Equation 1.11 | 12 |
| Equation 1.12 | 12 |
| Equation 1.13 | 13 |
| Equation 2.1 | 27 |
| Equation 2.2 | 27 |
| Equation 3.1 | 41 |
| Equation 3.2 | 41 |

ABBREVIATIONS AND SYMBOLS

| | |
|-------|--|
| 4-VP | : 4-vinylpyridine |
| AAEM | : Alkaline Anion-exchange Membrane |
| AFC | : Alkaline Fuel Cell |
| AEMFC | : Anion Exchange Membrane Fuel Cell |
| ATRP | : Atom Transfer Radical Polymerization |
| BPMFC | : Bipolar Membrane Fuel Cell |
| CHP | : Combined Heat and Power |
| DCFC | : Direct Carbon Fuel Cell |
| DFT | : Density Functional Theory |
| DMFC | : Direct Methanol Fuel Cell |
| DMSO | : Dimethyl Sulfoxide |
| DVB | : Divinylbenzene |
| ETFE | : Poly(ethylene- <i>co</i> -tetrafluoroethylene) |
| FC | : Fuel Cell |
| GL | : Graft Level |
| IP | : Immersion Precipitation |
| IPA | : Isopropanol |
| MCFC | : Molten Carbonate Fuel Cell |
| MFC | : Microbial Fuel Cells |
| NMR | : Nuclear Magnetic Resonance |
| OCV | : Open Circuit Voltage |
| ORR | : Oxygen Reduction Reaction |
| PA | : Phosphoric Acid |

| | |
|-------|---|
| PAFC | : Phosphoric Acid Fuel Cell |
| PBI | : Poly(benzimidazole) |
| PDI | : Polydispersity Index |
| PEFC | : Proton Exchange Fuel Cell |
| PEMFC | : Polymer Electrolyte Membrane (Proton Exchange Membrane) Fuel Cell |
| PSSA | : Poly(styrene sulfonate acid) |
| PSSS | : Poly(sodium styrene sulfonate) |
| PVDF | : Poly(vinylidene fluoride) |
| RH | : Relative Humidity |
| RIGP | : Radiation Induced Graft Polymerization |
| SOFC | : Solid Oxide Fuel Cell |
| SPEEK | : Sulfonated poly(ether ether ketone) |
| TAC | : Triallyl-cyanurate |
| TFE | : Tetrafluoroethylene |
| TGA | : Thermogravimetric Analyses |
| THF | : Tetrahydrofuran |
| TIPS | : Thermally Induced Phase Separation |
| UTM | : Universal Tensile Machine |
| VIPS | : Vapor Induced Phase Separatio |

1. INTRODUCTION

1.1. History of fuel cell

Luigi Galvani was the first person who discovered the field of electrochemistry. In his lecture on the 30th of October 1786, at the Academy of Sciences of Bologna, he presented the result of his study on animal electricity. By publishing Galvani's results a controversy with Alessandro Volta arose, who did not believe in animal electricity [1, 2]. The development of Volta's battery which was inspired by Nicholson and Bennet was another milestone in electrochemistry [3]. With the help of Volta's battery, Nicholson and Carlisle could electrolyze acid solution, and generate hydrogen and oxygen [4]. The most important contribution to electrochemistry and electromagnetism was obtained by Michael Faraday in his paper in 1821 that challenged the previous theories on electromagnetism. In his later work he could establish the basis of today's electrochemistry [5].

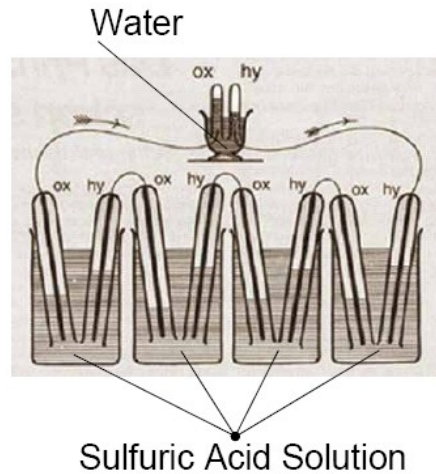


Figure 1. 1. Schematic of Sir William Grove fuel cell 1839 [6].

The first fuel cell can be attributed to Sir William Grove. In 1839 he could demonstrate that it is possible to generate electricity by passing the products of water electrolysis over the platinum electrodes (Figure 1.1). Later on in 1889, Mond and Langer became the first researchers who coined the term "Fuel Cell" (FC). They tried to scale up the Grove's cell for electricity production, but because of the poisoning of platinum catalyst by impurities in supporting gases,

and the high price of their FC, they could not scale up this technology. In the early 20th century there were some efforts made by Jacques to develop carbon batteries on the one hand, and fuel cell mechanism by Bacon on the other hand. The first Proton Exchange Fuel Cell (PEFC) was invented in 1955 by William Grubb at General Electric. Due to its low weight and compactness, it was first deployed by U.S. Gemini program in 1962 [7]. Since 1960s, FC technology faced many improvements and branched into different types of cells. Yet PEFC remained as one of the promising types of FC due to its high efficiency.

1.2. Types of fuel cells

Since the invention of the first fuel cell by Sir William Grove different types of FC systems have been developed, and they are categorized based on the fuel they use, the mechanism of ionic transportation, the type of material being used in them and other criteria. The feature which all the FC systems have in common is that they are all designed for energy conversion purposes. Figure 1.2 shows the FC technologies already developed based on their operating temperature, and Table 1.1 provides a detailed comparison between current FCs kinetics, theoretical efficiency, practical efficiency and the range of their operating temperatures (Polymer Electrolyte Membrane Fuel Cell (PEMFC), Direct Methanol Fuel Cell (DMFC), Alkaline Fuel Cell (AFC), Phosphoric Acid Fuel Cell (PAFC), Solid Oxide Fuel Cell (SOFC), Molten Carbonate Fuel Cell (MCFC), Direct Carbon Fuel Cell (DCFC)) [8].

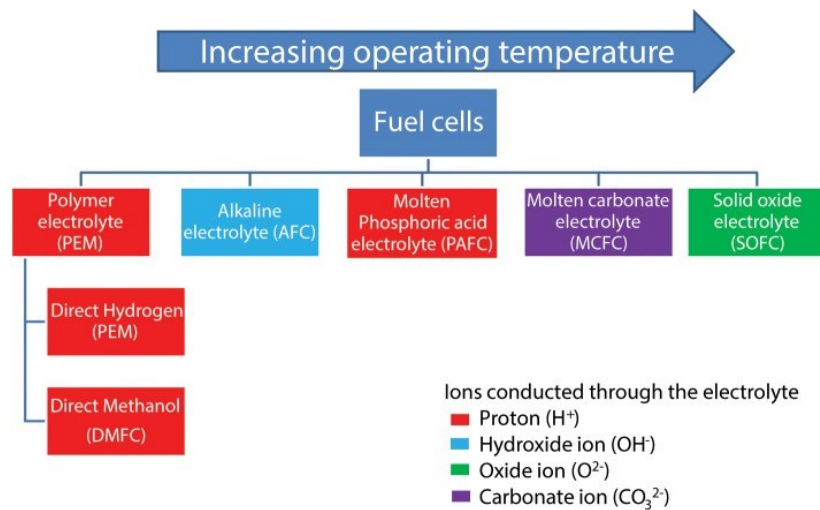


Figure 1. 2. Classification of current commercial fuel cell technologies [8].

The most common commercial fuel cells have actual efficiencies ranging from 40% to 60% aside from their operating temperature. Additionally, in the range of 80°C to 500°C only the PAFC type of fuel cell with 40% electrical efficiency is operational. In a fuel cell, the rest of chemical energy which doesn't convert to electrical energy is released as waste heat to environment. This heat energy can be partially utilized if consumed by a heat engine. According to Carnot Efficiency, the maximum achievable thermal efficiency for any heat engine is a function of the temperature of the heat source (T_{max}) and the ambient's temperature (T_{min}) (Equation 1.1). Therefore, high temperature fuel cells attracted more attention for Combined Heat and Power (CHP) systems (Table 1.1), which enables these systems to benefit from a higher overall efficiency [9, 10].

Table 1.1. Theoretical and actual efficiencies of different commercial fuel cells and their operating temperatures [8].

| Fuel cell type | Fuel | Overall reaction | Operating temperature (°C) | Theoretical efficiency (%) | | Actual system efficiency (%) | |
|----------------|--------------------|---|----------------------------|----------------------------|----------|------------------------------|-----|
| | | | | Electric | Electric | Electric | CHP |
| PEMFC | H ₂ | H _{2(g)} + 1/2 O _{2(g)} = H ₂ O _(l) | 60–80 | 83 | 45–50 | 80–90 | |
| PEMFC | NG | CH _{4(g)} + 2O _{2(g)} = CO _{2(g)} + 2H ₂ O _(l) | 60–80 | – | 35–40 | 80–90 | |
| DMFC | CH ₃ OH | CH ₃ OH _(l) + 1 1/2 O _{2(g)} = CO _{2(g)} + 2H ₂ O _(l) | 20–60 | 97 | 20–25 | n/a | |
| AFC | H ₂ | H _{2(g)} + 1/2 O _{2(g)} = H ₂ O _(l) | 70 | 83 | 45–60 | n/a | |
| PAFC | NG | CH _{4(g)} + 2O _{2(g)} = CO _{2(g)} + 2H ₂ O _(g) | 200 | – | 40 | 90 | |
| SOFC | NG | CH _{4(g)} + 2O _{2(g)} = CO _{2(g)} + 2H ₂ O _(g) | 600–1000 | 92 | 45–60 | 90 | |
| MCFC | NG | CH _{4(g)} + 2O _{2(g)} = CO _{2(g)} + 2H ₂ O _(g) | 650 | 92 | 45–55 | 90 | |
| DCFC | Carbon | C _(s) + O _{2(g)} = CO _{2(g)} | 500–1000 | 100 | 70–80 | 90 | |

Accordingly, it will be useful to discuss the current commercial and developing FC technologies based on their operating temperature.

$$\eta_{carnot} = 1 - \frac{T_{min}}{T_{max}} \quad (1.1)$$

1.2.1. Low temperature fuel cells

This category encompasses the types of FC systems which normally operate below 100°C. Among them, the application of Polymer Electrolyte Membrane, which is also known as Proton Exchange Membrane (PEMFC) dominates the other ones. PEMFC can be divided into two

distinct categories: the first one is known as Proton Exchange FC (PEFC) for Hydrogen FC as well as Direct Methanol FC (DMFC); and the second one is Anion Exchange Membrane (AEMFC) systems in which the membrane is only permeable to hydroxide anions. Some other technologies such as Bipolar Membrane (BPMFC) [11, 12], Laminar Flow Membrane-less FC [13], and Microbial Fuel Cells (MFC) [14, 15], which can be categorized as low temperature fuel cells, are still developing.

In case of PEFC, the membrane of FC assembly is only permeable to cations [16]. This feature is typically achieved by introducing some acidic functionality to the polymer material of the membrane. Therefore, once hydrogen, methane, or methanol is used as fuel only positively charged hydrogen ions are able to pass through membrane and complete the reaction. In contrast, in an AEMFC system, the membrane is only permeable to hydroxide ions which are negatively charged [17, 18]. This property is achieved by introducing basic functionality to the membrane which is also the reason why this type of membrane is also referred as Alkaline Anion-exchange Membrane (AAEM). In general, polymers which either have acidic or basic property are called Ionomers. Figure 1.3 shows the difference between PEFC and AEMFC systems.

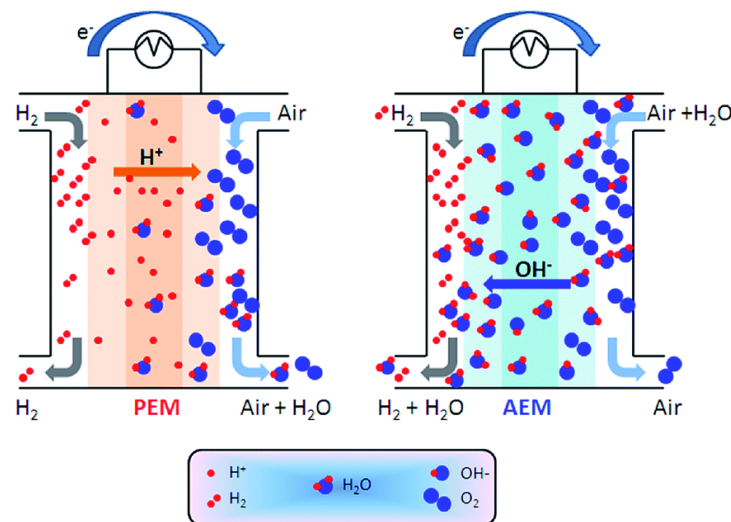


Figure 1. 3. Difference between two types of systems for FC [18].

1.2.2. Intermediate temperature fuel cells

Normally intermediate temperature for fuel cell application refers to the temperature gap between PEMFCs and SOFCs which is usually between 100°C to 600°C. This temperature range has many advantages over low temperature for FCs such as: minimizing catalyst poisoning by carbon monoxide (CO), reducing the requirement for noble metals as catalyst, improving the efficiency, and solving the fuel cell flooding problem [19]. Originally, alkaline fuel cells used alkaline metal hydroxides such as potassium hydroxide (KOH) for electrolyte. Thus, using alkaline metal hydroxides enabled them to operate at temperatures above 100°C, ranking them as intermediate temperature fuel cell [20]. In contrast, AFCs are very sensitive to the carbon dioxide (CO₂) contamination of electrolyte, which converts hydroxides to carbonates [21].

Another type of fuel cell which is able to work at an intermediate temperature range is phosphoric acid FC [22]. In PAFC, phosphoric acid is used as an electrolyte material and it can be retained with the help of an inorganic frame such as silicon carbide (SiC) [23]. In a very similar fashion, PAFC can be used with organic frames in order to retain phosphoric acid, and these types of membrane are usually referred to as high temperature (HT) PEMFC [24-28]. In HT-PEMFC, besides phosphoric acid, other high temperature ionomers such as poly(vinyl phosphonic Acid) is also used in the electrolyte structure to enhance the ionic conductivity at high temperature [29-34].

The other attractive type of fuel cell is based on solid acids which also fit into this category. Solid acids are monovalent or divalent metal cations combined with tetrahedral oxyanions [35] having the general form of $A_xH_y(XO_4)_{(x+y)/2}$ (X is Se or P, S, As and A is NH₄ or Cs, Ti, Li, K, Rb) [36]. The size of alkali metal ions directly influences the melting point and proton conductivity of the solid acids in such a way that as the size of cation increases the melting point of the solid acid increases as well. Therefore, many of the studies focused on Cs⁺ hydrates as a membrane capable of operating at temperatures as high as 250°C whether solely [37, 38], or in combination with other inorganic/organic materials [39-43].

1.2.3. High temperature fuel cells

Solid Oxide FCs (SOFC) are another type of fuel cell that are named based on the material being used as their electrolyte material, and are capable of operating between temperatures between 600°C and 1000°C. SOFCs, due to their high operating temperature, are one of the best candidates for CHP systems [10, 44]. Additionally, they can benefit from using nickel and nickel alloys as cheap substitute materials for the catalyst [45]. Although SOFC is a potential candidate to dominate the market, because of technical constraints limited their application only to the labs and prototypes. Some of these problems are: the extended start up duration, the use of expensive materials for operation at elevated temperatures, and the failure of the system due to thermal stress between the SOFC components (Figure 1.4) [46]. One approach to overcome these problems is lowering the cell temperature around 600°C or lower, which is referred to as Low Temperature (LT) SOFC. Some efforts are done by using Ceria-based materials such as CeO_2 , $Ce_xZr_{1-x}O_2$, and $Ce_{1-x}R_xO_{2-x/2}$ (R : rare earth) and isovalent-cation-stabilized bismuth oxides [47, 48], yet these types of material suffer from electrical conductivity and sintering problems [44]. Perovskites are a category of ceramics which maintain suitable ionic conductivity for LT-SOFC applications such as $BaCe_{0.8}Y_{0.2}O_3$ and $SrCe_{0.8}Y_{0.2}O_3$. The drawback of these ceramics is their instability under water vapor and CO_2 [49]. $BaZr_{0.8}Y_{0.2}O_3$ is a perovskite proton conductor material that has even higher conductivity than the aforementioned perovskites, and it is stable under vapor and CO_2 [50, 51]. $La_2Ce_2O_7$ is another ceria based material which also exhibits proton conduction for LT-SOFC applications [52].

Molten Carbonate Fuel Cell (MCFC) is a type of FC which uses molten alkali metal carbonates such as $LiCO_3$, $NaCO_3$, KCO_3 or a combination of them as electrolyte material, and has an operating temperature of around 650°C, and is capable of using different types of fuel. This type of fuel cell can benefit from using metal catalysts such as alloys of nickel including NiCr and NiAl. One of the challenges of MCFCs is the corrosion of electrode material which limits their operation life despite their high efficiency and low cost [53]. Direct carbon fuel cell (DCFC) is another type of FC which operates at temperatures above 600°C, and it is the only FC that operates on carbon as a solid fuel. The theoretical efficiency of this type of FC is 100% and due to its high efficiency, it is considered a possible substitute for coal-burning power plants [54]. Most of DCFC designs are based on SOFC, MCFC, or molten hydroxide electrolytes [55, 56].

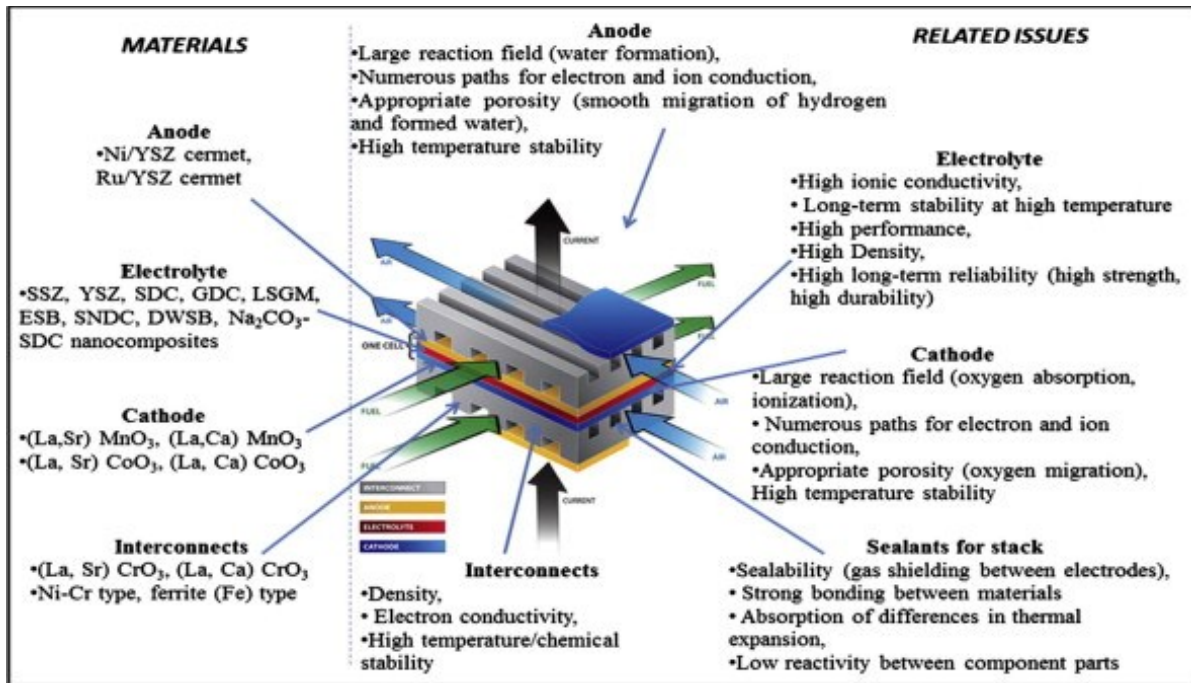


Figure 1. 4. Materials and related issues for SOFC [46].

1.3. Governing principles for proton exchange fuel cell

The process of oxidation and reduction in PEFC can be simplified through its half-cell reactions. The most ideal case would be the chemical reactions of hydrogen and oxygen and their relevant electron transfer. Equations 1.2 and 1.3, respectively, show the ionization reaction for H₂ and O₂ in a PEFC, and consequently after the electron transfer a water molecule forms (Equation 1.4).



Once hydrogen and oxygen are directly in contact, this electron transfer between the two atoms causes combustion and heat generation in the reaction medium, and the generated electricity is not utilizable. To utilize this electricity, as an alternative method of reaction, the two half-cell reaction can occur on separate catalysts, and the ions will be able to combine to form the reaction product later on. Norskov et al. performed a tremendous amount of research to better understand the behavior of heterogeneous catalysts through density functional theory (DFT) and empirical experiments [57-62]. The catalyst activity comprises two main processes: chemical adsorption (chemisorption) and desorption. In the chemisorption, the molecule first binds with the s-band orbital of catalyst and goes through hybridization. Depending on the electron filling of the orbitals with respect to the Fermi level, the energy of bonding and anti-bonding can be determined. In case of transition metals with d-band, the hybridization will also be affected by the electron filling of these orbitals with respect to their Fermi level in such a way that as we move from the left side of periodic table toward the right side, the chemisorption decreases and the desorption increases. This trend leads to an optimum catalyst activity for different elements for specific reaction and enthalpies. For example, in the oxygen reduction reaction (ORR) at low temperature Pt is the closest element to the maximum catalyst activity, while at higher temperature Ni depicts the highest activity for ORR [63].

Spillover is a process in which after a molecule undergoes decomposition on the surface of a heterogeneous catalyst, the resulted products of catalyst activity go through a surface diffusion process [64]. The diffusion process is mainly a function of surface properties, as well as ionic concentration. Therefore, the diffusion of ionic species not only occurs on the catalyst itself, but also on the catalyst supporting material. In the case of catalytic reactions, in which electron donation and acceptance of reactants happen on the same surface, the reaction can continue until the reactants are consumed. In contrast, in a FC catalytic reaction, since electron donation and acceptance are occurring on separate catalysts, the limiting parameter for reaction is determined by the formation of a double layer of generated ions with respect to the electrode potential. Since the catalyst material and the reactants all have different Fermi levels, as they get in touch with each other, they establish a potential difference which will lead to the generation of an electrical field around the catalyst [65].

In order to complete the reaction, the generated ions on the surfaces of catalysts must be able to reach each other to form the reaction product. Since these ions are still attached to the surface of the catalyst by means of electrostatic forces, therefore no reaction will occur unless these ions can be separated from the catalyst and travel through a medium. The process of separation of ions from the surface occurs through electron exchange between two electrode catalysts. Due to their opposite electrical charges, one electrode donates electrons (i.e. anode) and the other electrode accepts electrons (i.e. cathode). In the case of water formation, the oxidation of hydrogen molecule on anode releases two electrons. On the other hand, ORR on cathode requires two electrons for each oxygen atom (equations 1.2 and 1.3). If there is no electrical potential between two electrodes by connecting them electrically together, or applying an electrical load, the electrostatic force between ions and catalyst surface will decrease, and ions are free to travel to form water.

In order to utilize the electrical energy of the reaction the medium in which ions travel must be electrically insulating while at the same time remaining ionically conductive. Ionic conduction can occur in plasma [66], gases [67], supercritical fluids [68], liquids [69], and solids [70]. The movement of ions in the medium is based on the principles of mass transfer. In general, the modes of mass transfer contain:

- 1- *Migration (drift)*: movement of particles in the medium by exerting electrical field.
- 2- *Diffusion*: movement of species due to the gradient of chemical potential in the medium.
- 3- *Convection*: movement of species by natural or forced convection of the medium (applies only to fluids).

These phenomena in electrochemistry are abbreviated in the Nernst-Planck formula, the one-dimensional form which is expressed by Equation 1.5, in which J_i is the flux of ions i in x direction ($mole/s.cm^2$), D_i is the diffusion constant (cm^2/s), $\partial C_i(x)/\partial x$ is the concentration difference, $\partial \phi(x)/\partial x$ is the potential difference, Z_i is the charge (*dimension-less*), C_i is the concentration ($mole/cm^3$) of ions i , and $v(x)$ is the speed (cm/s) with which a unit of volume in solution moves along the x direction [71].

$$J_i(x) = -D_i \frac{\partial C_i(x)}{\partial x} - \frac{Z_i F}{RT} D_i C_i \frac{\partial \phi(x)}{\partial x} + C_i v(x) \quad (1.5)$$

From an overall point of view, the purpose of a fuel cell is converting the chemical energy of reactants into electrical energy. Therefore, it is possible to define the theoretical efficiency of fuel cells as the fraction of attainable electrical energy with respect to the chemical potential energy of reactants (Equation 1.6).

$$\eta_{max} = \frac{\Delta G}{\Delta H} \quad (1.6)$$

In this equation η_{max} is the maximum attainable efficiency, ΔH is the change of enthalpy (*Joule*) for reactants and reaction products, and ΔG is the change in Gibbs free energy (*Joule*) which is defined as follow (Equation 1.7):

$$\Delta G = \Delta H - T\Delta S \quad (1.7)$$

In this formula T is the temperature (K°) and ΔS is the entropy (*Joule/K $^\circ$*) or the irreversibility of the system. Theoretically, the efficiency of a fuel cell will increase as the operating temperature decreases. This is due to the fact that at a higher temperature more of the available enthalpy converts to heat rather than to electrical energy. The efficiency of fuel cells is also directly related to the change in Gibbs free energy through the Equation 1.8.

$$\Delta G = -nFE \quad (1.8)$$

In this equation, n is the number of electrons involved in the formation of reaction products (for equation 1.4, $n = 2$), F is Faraday constant ($F = eN_A$, e is the electron charge, N_A is the Avogadro's number), and E is the cell potential or electromotive force (EMF), the calculated values for hydrogen FC with respect to temperature are presented in Table 1.2 [72].

Table 1. 2. The effect of operating temperature of hydrogen fuel cell on the cell voltage and maximum efficiency[72].

| Form of water product | Temp °C | $\Delta\bar{g}_f$, kJ mol ⁻¹ | Max EMF V | Efficiency limit % |
|-----------------------|---------|--|-----------|--------------------|
| Liquid | 25 | -237.2 | 1.23 | 83 |
| Liquid | 80 | -228.2 | 1.18 | 80 |
| Gas | 100 | -225.2 | 1.17 | 79 |
| Gas | 200 | -220.4 | 1.14 | 77 |
| Gas | 400 | -210.3 | 1.09 | 74 |
| Gas | 600 | -199.6 | 1.04 | 70 |
| Gas | 800 | -188.6 | 0.98 | 66 |
| Gas | 1000 | -177.4 | 0.92 | 62 |

Although it seems that at lower temperature the hydrogen fuel cell has more efficiency, in case of methane (CH₄) as fuel, the change in Gibbs free energy is less pronounced, leading to an almost constant voltage at different operating temperatures. Some of the oxidation pathways of methane are shown in Figure 1.5 [73].

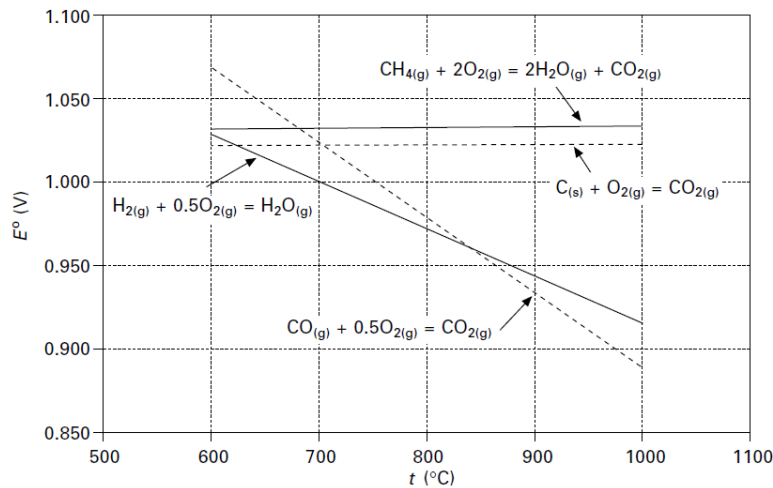


Figure 1. 5. The effect of temperature vs. cell voltage $E^\circ(v)$ for hydrogen and methane as fuel [73] .

In a practical fuel cell, the thermodynamic efficiency of the cell is influenced by some additional losses (overpotentials). The activation (or polarization) overpotential is the major loss in a fuel cell which is the reduction of cell potential due to the rate of electron transfer of surface reactions and can be explained by Tafel (Equations 1.9 and 1.10), or alternatively by Butler–Vollmer formula (Equation 1.11).

$$\Delta V_{act} = A \ln \left(\frac{i}{i_0} \right) \quad (1.9)$$

$$A = \frac{RT}{2\alpha F} \quad (1.10)$$

$$i = i_0 \exp \left(\frac{2\alpha F \Delta V_{act}}{RT} \right) \quad (1.11)$$

ΔV_{act} is the difference between open circuit voltage (OCV) (V) and the voltage after current i (A/m^2) passes through the electrode, i_0 is the threshold current (A/m^2) which OCV starts to drop, α is the charge-transfer constant which relies on reactants and the selection of materials for electrode, T is the temperature in Kelvin (K°), F is the Faraday coefficient, and R is the ideal gas constant ($Joule/K.mole$). The activation overpotential can be reduced by increasing the working temperature of FC, choosing correct materials for electrodes, maximizing the catalyst surface area, and increasing the concentration of reactants or their pressure. The other loss in a fuel cell is ohmic overpotential (ΔV_{ohmic}), which is the resistance of ionic conductive medium toward moving ions, and the electrical resistance in the electrical connections of the cell (Equation 1.12).

$$\Delta V_{ohmic} = ir \quad (1.12)$$

In this formula i is the current density (A/cm^2) and r is the resistance per surface area (Ω/cm^2). In order to minimize the ohmic loss, the ionic conductive medium should have a minimum resistance, all electrical connections to the electrodes must be sufficiently conductive, and the distance between two electrodes must be minimized.

$$\Delta V_{trans} = m \exp(ni) \quad (1.13)$$

Another loss is the concentration (or mass transport) overpotential due to the reduction in concentration of reactants which is directly related to the reduction of their partial pressure. This phenomenon happens by blocking the supply of reactants which, in case of air, the presence of nitrogen reduces the oxygen concentration at high currents, or in case of hydrogen fuel cell concentration overpotential occurs by accumulation of water at electrode-gas interfaces. The concentration overpotential can be calculated by means of Equation 1.13 in which m is typically about $3 \times 10^{-5}(V)$, and n about $8 \times 10^{-3}(m2/A)$ [72]. There are also cross-over and mixed potential losses as a result of passing non-ionized species through the conductive medium, electrical conductivity between two electrodes, and side reactions such as Pt-O bond formation in case of hydrogen fuel cell [74].

The overall effect of these losses for an empirical fuel cell is shown in Figure 1.6, and it can be observed that as the current-density elevates the fuel cell voltage drops in four distinctive regimes.

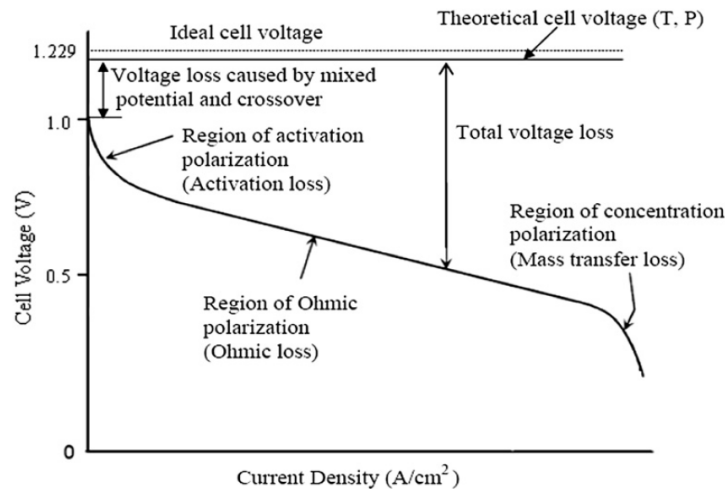


Figure 1. 6. Typical performance of a hydrogen fuel cell and the effect of common overpotentials [73].

1.4. Proton exchange membranes

Proton exchange membranes, also known as polymer electrolyte membranes (PEM), are in general referred to any ionic conductive electrolyte which conducts only positively charged ions, which, in the case of a hydrogen ion, is called a proton. As already discussed, some ceramics also exhibit proton conduction, but normally PEMFC is a low temperature FC which uses polymer materials as electrolyte. Proton is the only ion which does not have any electron in its orbitals, and as a result this cation has its own unique properties. It is believed that there are two types of mechanisms involved in proton conduction: one is the vehicle mechanism in which a proton in an aqueous system forms a hydronium ion (i.e. H_3O), and the other one is the Grotthuss or hopping mechanism in which protons hop from one molecule to the other one [75]. As a proton hops from one oxygen site to another it faces a potential barrier which is a function of distance. For infinitesimal distances, the electron orbitals of donor and acceptor hybridize to such a value that the barrier completely disappears (Figure 1.7) [76].

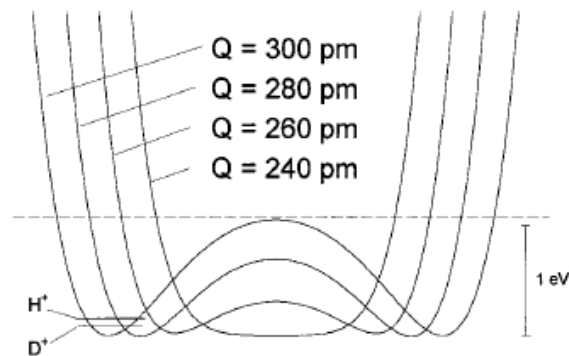


Figure 1. 7. Semiempirical potential energy for proton transfer across hydrogen bindings of symmetrical conformations of the type R-O-H...O-R for different oxygen distances Q and full stabilization of the surrounding [76].

The polymer electrolytes are usually non-homogeneous, and there are regions of non-conductive and ionic-conductive channels [77, 78]. Therefore, the arrangement and connectivity of these ionic channels also affect the proton conductivity of PEM. The hopping mechanism is not limited to water, but also some acids such as phosphoric acid, which has the highest proton conductivity among the other substances, also owes 98% of its proton conductivity to Grotthuss mechanism [79, 80]. As a result, hydrated polymers with acidic groups are considered the most suitable PEM structure. In contrast, by reducing the level of hydration the proton conductivity of

PEM also reduces up to the point that at 0% relative humidity the proton conductivity is almost negligible [81]. For example, in case of poly(vinyl phosphonic acid) (PVPA) simulations suggest that in comparison with phosphoric acid, the dominant mechanism for proton conductivity in PVPA is a short distance vehicle mechanism of hydronium ion between the acid sites of the polymer [82] (Figure 1.8).

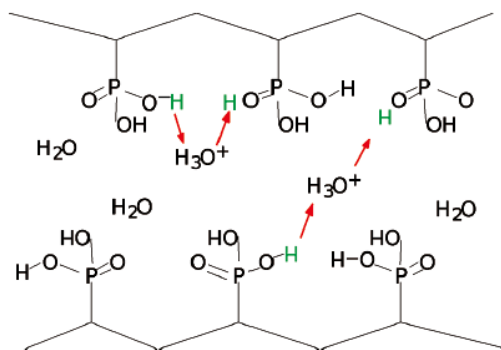


Figure 1. 8. Grotthuss-type mechanism by means of hydronium ions in poly(phosphonic acid)[82].

For applications in which the operating temperature of FC is higher than 100°C the relative humidity decreases, and maintaining the relative humidity at elevated temperatures requires increasing the FC operating pressure. The proton conductivity at elevated temperatures can be addressed by means of an acid-base type of salts. The Walden rule indicates that the ionic conductivity is inversely proportional to the viscosity of the electrolyte [83]. Considering the solid nature of an acid-base PEM, and according to the Walden rule it is expected that there is no ionic conductivity for solid salts. In contrast, some researches have proven that the Walden rule does not apply to polymeric systems [84, 85]. One of the HT-PEM systems which has been well studied is the polybenzimidazole (PBI)-phosphoric acid (PA) system [27]. Experimental and theoretical studies imply the fact that the proton conductivity in the case of acid-base membranes relies on different mechanisms (Figure 1.9). These studies suggest that proton conduction depends on the interactions between PBI-PBI, PA-PA, PBI-PA, PBI-water and PA-water [86-89].

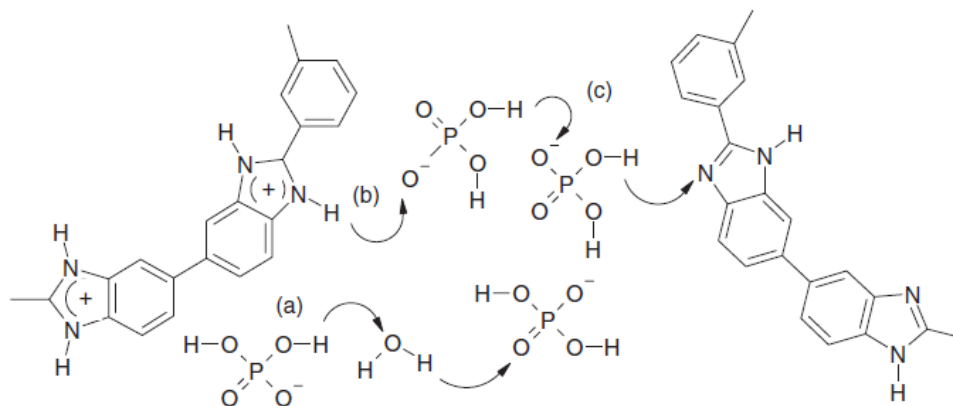


Figure 1. 9. Proton conductivity system for acid doped PBI-membrane [27].

1.4.1. Fluorinated proton exchange membranes

It is possible to use a variety of polymer electrolytes for the FC application. One branch of these materials is based on fluorinated or partially fluorinated membranes. Instead of having a C-H bond like hydrocarbons, these types of polymers have a C-F bonding in their structure, and therefore they are also referred to as fluorocarbons or fluoroplastics. The substitution of hydrogen with fluorine brings some changes in the physical and chemical properties of the polymer due to the difference in their electronegativity and molecular weight. As an example, polytetrafluoroethylene (PTFE) is a linear polymer similar to polyethylene (PE), but PTFE has a higher melting point, a higher chemical resistivity, and a larger free volume due to its helical molecular structure with respect to the zigzag structure of PE [90, 91].

During the past decade Nafion[®] produced by DuPont as the most successful PEM material has been owing its superiority because of its fluorinated polymer structure. This material is essentially a fluorocarbon with attached sulfonic acid groups. Being similar to Teflon[®], Nafion[®] exhibits an excellent resistance to chemical attacks and an extremely low release rate of degradation products into the surrounding medium. It also has a relatively high operation temperature range, and may be used in many applications at temperatures up to 190 °C. Nafion[®] has a high proton conductivity and acts as a superacid catalyst because its sulfonic acid groups act as an extremely strong proton donor. The interaction of sulfonic acid groups with water results in rapid water absorption and water transport through the Nafion[®] material [16].

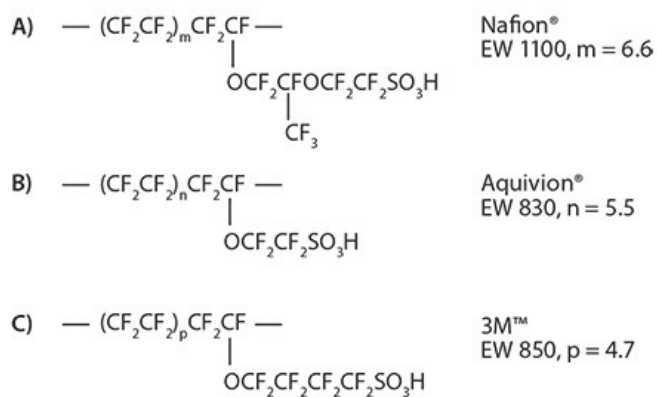


Figure 1. 10. A) Nafion® B) Aquivion® C) 3M structures [92].

Even though Nafion® has dominated the market, there are some drawbacks associated with Nafion®, some of which include: high manufacturing cost, low conductivity for high temperature applications and loss of chemical and mechanical stability at elevated temperatures. Besides Nafion®, there are some other similar products offered by different companies such as Solvay® (Aquivion®) and 3M (Figure 1.10) [92]. Though all of these membranes have a very similar polymeric structure, they have different synthesizing routes.

The process of synthesizing Nafion® and Aquivion® starts with a tetrafluoroethylene (TFE) monomer in gaseous form, and then it reacts with sulfur trioxide (Figure 1.11) [93]. After the completion of both pathways the result is a perfluoro(alkylvinyl ether) with a sulfonyl acid fluoride monomer. The polymerization of this monomer with TFE will result in a brushed-like fluorinated polymer with sulfonic acid groups [94]. In contrast, 3M developed a membrane through electrochemical fluorination of a hydrocarbon material (Figure 1.12) [95]. Since the radical-attack on the acidic end-groups of the polymer backbone is the main cause of polymer damage [96], the resulted polymer is further stabilized by post-synthesis fluorination.

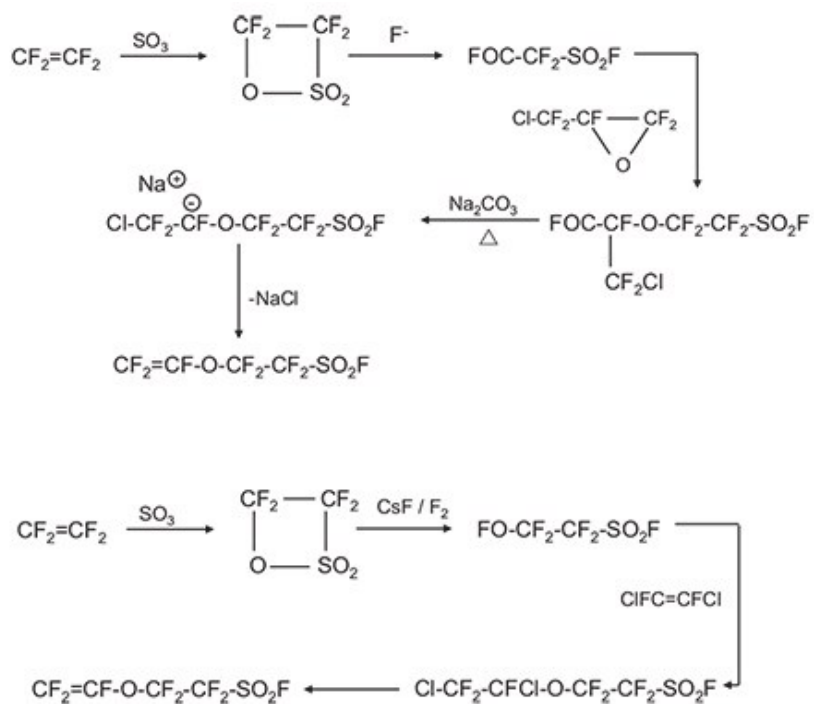


Figure 1. 11. Different synthesis pathways for perfluoro(alkyl vinyl ether) with sulfonyl acid fluoride, above) DuPont method for Nafion[®], below) Solvay method for Aquivion [93].

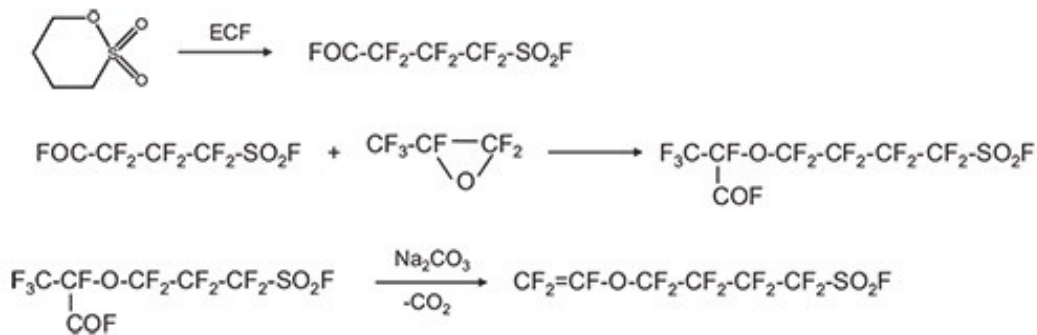


Figure 1. 12. 3M method for synthesizing perfluoro(alkylvinyl ether) with sulfonyl acid fluoride monomer [95].

1.4.2. Sulfonic polymers and processes

The addition of acidic groups to monomers or polymers is an essential step in membrane functionalization. Among the variety of acidic groups in hydrocarbons, sulfonic groups, which are a result of sulfonating polymers and monomers, have been the center of attention for the synthesis of non-fluorinated PEM systems. The sulfonic groups can be introduced by means of the reaction of a sulfonating agent with hydroxyl or aromatic groups of hydrocarbons. The earliest type of sulfonic polymer that was used in the Gemini program was a cross-linked polystyrene sulfonic acid (PSSA) which had a short life due to oxidative stress [97]. Despite the initial failure of PSSA membranes, the effort to improve the properties of aromatic polymer membranes for applications below 60°C still continues.

The sulfonation of polymers, usually referred to as post-sulfonation, is usually done by sulfonating agents such as: concentrated sulfuric acid, fuming sulfuric acid (oleum), chlorosulfonic acid, acetyl sulfate, sulfur trioxide complexes and trimethylsilyl chlorosulfonate ((CH₃)₃SiSO₃Cl). Some of the post-sulfonated aromatic polymers include: sulfonated styrene copolymers [98, 99], sulfonated polyimides (SPIs) [100], sulfonated poly(phenylene)s [101], sulfonated poly(arylene) types polymers [102] and sulfonated poly(phosphazene)s [103, 104]. Among the post-sulfonated aromatic polymers, sulfonated poly(ether ether ketone) (SPEEK) is one of the most outstanding materials for membrane applications (Figure 1.13) [105]. In these systems the degree of sulfonation can be controlled by changing the concentration of the sulfonating agent, temperature or reaction time.

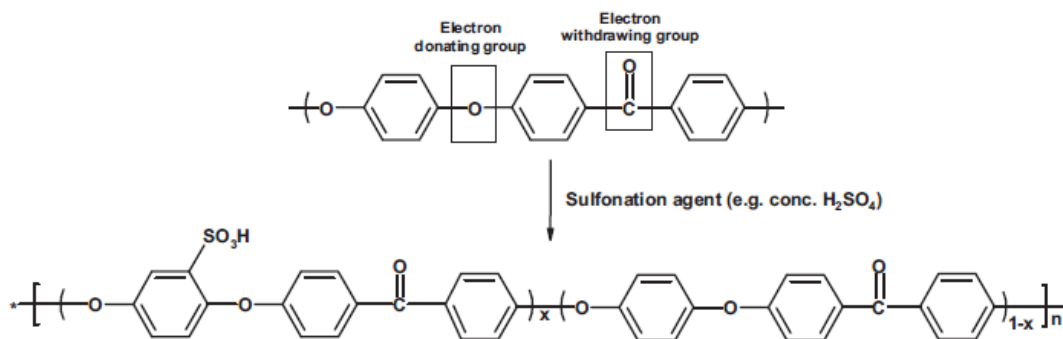


Figure 1. 13. Sulfonation of (PEEK) by sulfuric acid [106].

The alternative method used for synthesizing sulfonated aromatic membranes is polymerization of monomers with a sulfonic group. Some of the possible sulfonated aromatic monomers for PEM application include: sulfonated 4,4'-dichlorodiphenyl sulfone [107], 3,3'-disulfonated 4,4'-difluorodiphenyl ketone [108], 3,3'-disulfonated 4,4'-dichlorodiphenyl sulfone [109, 110], 4,4'-diamino-biphenyl 2,2'-disulphonic acid (BDSA) [100, 111-113]. The abovementioned monomers are the ones suitable for condensation polymerization. Additionally, one may also use a vinyl type of monomers such as sodium styrene sulfonate (SSS) in radical polymerization applications.

1.4.3. Radiation induced graft polymerization

Grafting is a process in which a polymer is added to another polymer or substrate. There are two methods of grafting, *grafting-from* and *Ggrafting-onto* systems. Both of these systems will lead to brushed-like polymer structures. In the *grafting-onto method*, the functional group at the end of a polymer reacts with a reactive site on a polymer with multiple reactive sites. On the other hand, in the *grafting-from method*, polymerization occurs on a polymer backbone with multiple active radical sites. These sites act as an initiator for radical polymerization, and therefore the second polymer polymerizes from the backbone of the other polymer. Another option for synthesizing brushed-like polymers is *grafting-through* by using a monomer which already contains a long chain polymer attached to a vinyl group (Figure 1.14) [114].

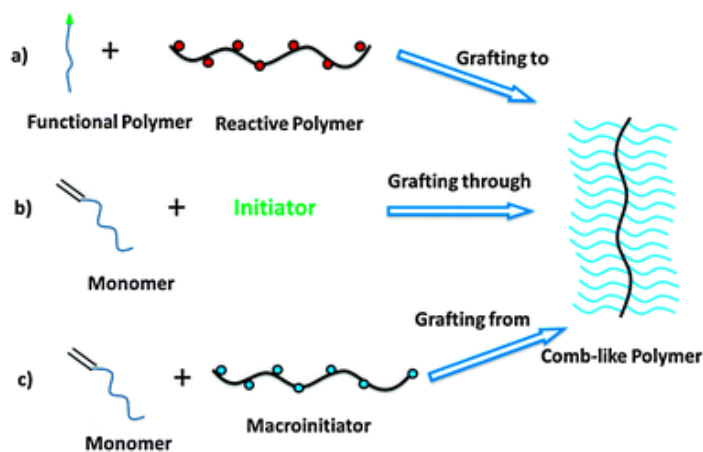


Figure 1. 14. Methods for preparing comb-like polymers: (a) “Grafting-onto” (b) “Grafting-through” (c) “Grafting-from” [114].

Radiation induced graft polymerization (RIGP) is a *grafting-from* type of polymerization in which active sites are generated by radiation. The received radiation dose is defined as the energy passed through the material in Gray (Gy) or kilo Gray (kGy). The number of generated active sites is proportional to the amount of radiation dose that the material received [115-132].

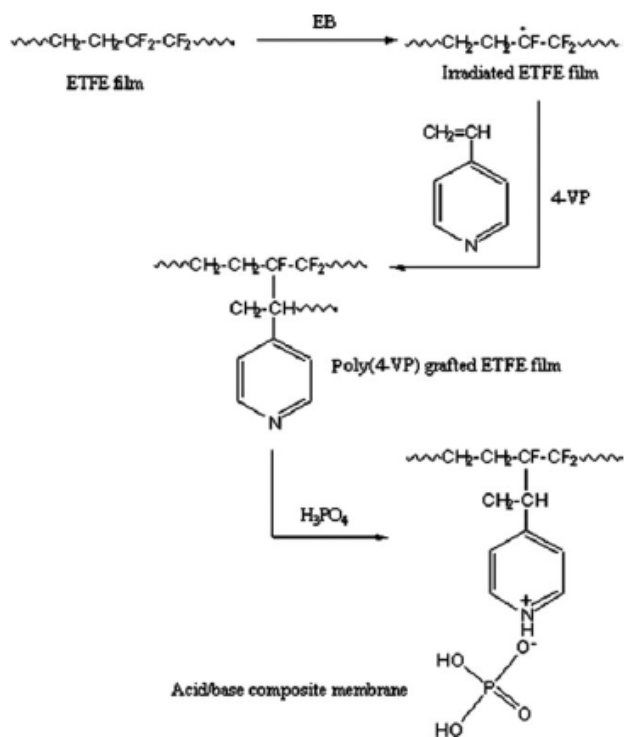


Figure 1. 15. Plausible mechanism of preparation of phosphoric acid doped poly(4-VP) grafted ETFE membrane [133].

The RIGP process can be performed as pre-irradiation and simultaneous-radiation polymerization [127]. Since radiation passes through all the polymers, therefore active sites can form on the polymer backbone whether it is a hydrocarbon or a fluorocarbon. This advantage brings the opportunity to benefit from chemical, mechanical, and thermal stability of fluorinated polymers, and at the same time using commercial vinyl-monomers in solution radical polymerization system to develop partially fluorinated membranes. Fluorinated polymers such as poly(tetrafluoroethylene-*co*-hexafluoropropylene) (FEP), poly(vinylidene fluoride) (PVDF), poly(ethylene-*co*-tetrafluoroethylene) (ETFE) poly(tetrafluoroethylene-*co*-perfluoropropylvinyl

ether) (PFA) and poly(tetrafluoroethylene) (PTFE) are the most common substrate material for fuel cell membrane applications [134]. Different combinations of polymers for low temperature PEM applications such as: ETFE-*g*-Poly(trifluorostyrene) [130], ETFE-*g*-Poly(styrene sulfonic acid) [124], ETFE- *g*-Poly(styrene sulfonic acid-*co*-acrylonitrile) [124], ETFE-*g*-Poly(α -methylstyrene-*co*-acrylonitrile) [135] as well as for AAEM applications [136-138] have developed with comparable ionic conductivity with respect to Nafion[®]. For HT-PEMFC applications, RIGP provides a simple and applicable method to develop high temperature membranes, and most of these studies are focused on acid-base type grafted fluorinated polymers with vinyl-monomers containing amine groups such as vinylpyridine and vinylimidazole (Figure 1.15) [133].

2. NANO-STRUCTURED POLY(VINYDENE FLUORIDE) GRAFT POLYSTYRENE SULFONIC ACID FOR PROTON EXCHANGE MEMBRANE

Research Objectives

The Fluorinated Nafion[®] membranes produced by DuPont are the dominant type of membranes used for Hydrogen fuel cell applications. These membranes are very expensive, and as a result it is one of the obstacles for realizing the Hydrogen as an alternative source of energy. Therefore, the main goal of this chapter is the development of an alternative proton exchange membrane for fuel cell applications which expresses similar characteristics to Nafion[®]. Styrene sulfonic acid is the sulfonated styrene monomer which is in sodium salt form, and it can be easily polymerized to obtain highly proton conductive polymers. Co-polymerization of poly(sodium styrene sulfonate) from poly(vinylidene fluoride) powder (which is a fluorinated polymer) by using radiation graft polymerization is considered to develop suitable proton conducting material for hydrogen fuel cell for the first time. Additionally, a facile method used for the modification of nano-structure of the membranes by means of vapour induced phase separation during casting process is considered to modify the morphology of ionic-channels. After the casting process ends the obtained membranes can be activated in an acidic aqueous solution and ready to be used in a fuel cell.

2.1. Introduction

The role of fossil fuels in the immense technological development undertaken during the last century is indisputable, and after almost a century, they are the main source of manmade energy supply. Currently, as the energy demand is remarkably increasing, the main concern is targeting the depletion of fossil fuels as well as its environmental. Among many developments in the field of energy conversion, the proton exchange membrane fuel cell (PEMFC) is one of the most promising candidates meeting many of the criteria as an alternative energy resource. However, one main obstacles of the PEM fuel cell is the manufacturing cost of its fully fluorinated proton exchange membrane that comprises 32% of the cost of PEMFC [139].

The first commercially available polymer electrolyte membrane (PEM), which still dominates the market, is Nafion[®] that is a perfluorosulfonic acid membrane. However, perfluorosulfonic acid membranes have a high manufacturing cost due to their complex fluorine chemistry. A variety of polymer formations have been proposed as an alternative for perfluorosulfonic acid membranes including: sulfonated poly(styrene), sulfonated poly(imide), poly(phosphazene), poly(benzimidazole), poly(arylene ether), poly(sulfone), poly(sulfoneether) and poly(phenylsulfone) [16]. Radiation induced graft polymerized sulfonic acid membranes are one of the best alternatives to Nafion[®] due to the advantages of their preparation method, ease of control over tailoring the membrane properties, as well as their low cost [115-118, 120, 122-127, 129, 130].

In radiation induced graft co-polymerization, the polymer film can be radiated by means of high energy electron beam or gamma ray. As a result of radiation, active radicals on the polymer backbone are formed. Therefore, the copolymerization process can be initiated from these radicals [122, 140]. Traditionally, styrene is incorporated to fluorinated polymers by radiation-induced grafting, and later the graft copolymer is sulfonated by means of a sulfonating agent [141]. This method for PEM preparation is known as the two-step radiation induced graft copolymerization in literature.

Radiation grafted sulfonic acid membranes are usually prepared by the radiation-induced grafting of the styrene monomer onto the partially fluorinated polymer films (such as ETFE, FEP, PVDF). Partially fluorinated polymers are also known for their high mechanical, thermal

and chemical resistivity. Among fluorine based polymers, poly(vinylidene fluoride) (PVDF) exhibits high mechanical strength, good chemical resistance and thermal stability as well as aging resistance to withstand to fuel cell conditions. Moreover, PVDF demonstrates good processability, and it is also soluble in common solvents [142]. PVDF-based micro-porous membranes are usually prepared by means of the controlled phase separation of polymer solutions into two phases. This transformation can be accomplished in several different ways, namely: (a) thermally induced phase separation (TIPS); (b) controlled evaporation of solvent from three component systems; (c) vapour induced phase separation; and (d) immersion precipitation (IP) [143]. Li et al. investigated the effect of water vapour on PVDF-dimethylformamide (DMF) solution system for relative humidity(RH) ranging from 0% to 60% at room temperature [144]. In their report they concluded that at 60%RH the PVDF goes through a phase separation in DMF and forms particles in micron and sub-micron sizes.

Lehtinen et al. and Slade et al. studied the graft copolymerization of styrene from the PVDF film, and later Lu et al. studied PVDF powder instead of PVDF film via the two-step radiation induced graft copolymerization [145-147]. However, one main disadvantage of the two-step radiation induced graft copolymerization is that the high degree of sulfonation cannot be achieved without damaging the grafted membranes due to the strong sulfonating agent/solvent media. Instead sulfonated monomers, such as sodium styrene sulfonate (SSS), can directly introduce the pentant sulfonic acid groups to the graft copolymer. Kim et al. used the direct grafting of SSS on the PVDF powder through the atom transfer radical polymerization (ATRP), while Su et al. applied the same system through redox initiation [148, 149], and finally radiation induced graft polymerization was used by Kim et al. and Nasef et al. [150, 151]. This method, which is also referred to as the single-step graft polymerization, has advantages in terms of simplification of synthesis process, increase of sulfonation efficiency, as well as reduction of production cost in comparison to the two-step graft polymerization method[141].

Previously, Nasef et al. studied the effect of pH and various type of acids over polymerization kinetics, and it was demonstrated that the pH of solvent system has a drastic effect on the polymerization level [152]. Additionally, in their study, it has been shown that sulfonic acid led to higher graft levels compared to other acids (such as HCl, HNO₃, CH₃COOH).

In this study the radiation-induced graft polymerization of SSS to PVDF powder was studied. For the first time in literature, the powder form of PVDF was chosen in order to increase monomer diffusion through the polymer backbone. An aqueous dimethyl sulfoxide (DMSO) solution, as a less hazardous system, was suggested, and its kinetics has been studied by means of NMR spectroscopy. The resulting powder was dissolved in DMSO [149], and cast as a thin film by means of the tape casting method in order to have a high quality and homogenous and dimensionally stable cast membranes, and was further modified by VIPS method to form a high porosity membrane. The PVDF-*g*-PSSA proton exchange membranes were studied in details for fuel cell related properties including *ex-situ* proton conductivity, water up-take, mechanical and thermal properties in comparison to Nafion[®] NR-211.

2.2. Experimental

2.2.1. Material

High molecular PVDF powder (Mw 380,000) was obtained from Solef, and Sodium 4-vinylbenzenesulfonate (90%), DMSO (99.5%), H₂SO₄ (97%), HCl(38%), Methanol (99.9%) were all purchased from Sigma Aldrich. All the materials were reagent grade and used as they were received without any further purification. De-ionized water with 18MΩ resistivity was used during the synthesis and conditioning of graft copolymers during the study.

2.2.2. Radiation induced graft copolymerization

The PVDF powder was weighted, and packed in small polyethylene plastic bags. The irradiation process was performed in γ -rays via ⁶⁰Co source at 50 kGy total irradiation dose and at room temperature. After irradiation, the PVDF polymer was kept in deep freeze. The polymerization performed in the 1.5 mole/L SSS aqueous solution of DMSO with PVDF/SSS w:w ratio of 1:3, water/DMSO v:v ratio of 1:4, and sulfuric acid concentration of 0.2 mol/L. The prepared solution was degassed with N₂ for 30 minutes, and was then left at 60°C in different reaction time. After the grafting process, the resulted polymer was precipitated with acetone first and then

further precipitated with methanol, washed with water and filtered, and dried in oven for 24 hours at 60°C.

2.2.3. Membrane preparation

The obtained graft copolymers with different graft levels were dissolved in DMSO with 15% wt.% ratio at 105°C, and were then degassed in vacuum and cast over a glass plate by means of the tape casting method. In order to obtain nano-structured morphology in the membranes, they were exposed to 60%RH in air atmosphere until the cast solution became opaque through VIPS process. Later on, the samples were left in the vacuum oven at 180°C until they were shaped into a 40µm thick thin film. It should be noted that the temperature was considered in such a way as to be higher than the melting point of PVDF, but below the boiling point of DMSO in order to achieve better mechanical properties similar to melt casting membranes. The resulted films were activated in 1 M hydrochloric acid at 60°C for 12 hours, and then washed with deionized water for several times prior to use.

2.2.4. Characterization of membranes

The ¹H-NMR (VARIAN INOVA AS500) was used to determine the number of hydrogen atoms in the phenyl group of PSSS in comparison to the number of hydrogen atoms in PVDF by means of measured molar ratios. The graft level of polymer was calculated through Equation 2.1:

$$Graft\ level = \frac{W_g - W_o}{W_o} \times 100 \quad (2.1)$$

where W_g and W_o are the weights of grafted and pristine PVDF powder, respectively. The water up-take of membranes was measured by comparing the weight of fully humidified membranes with respect to their dry weight. After activating the membranes, they were soaked in water for 24 hours, and later on the extra water on the membranes was wiped with tissue paper, while their weight was measured immediately. The water up-take was calculated through Equation 2.2:

$$\text{Water uptake} = \frac{W_h - W_d}{W_d} \times 100 \quad (2.2)$$

where W_h and W_d are the weights of humidified and dry membranes, respectively. Additionally, the proton conductivity of the membranes was tested in the Becktech 4-point probe conductivity device at room temperature and 100% humidity. Thermogravimetric analyses (TGA) of the samples were performed by Shimadzu DTG-60H, in comparison with Nafion[®] NR-211, under the nitrogen atmosphere with the increment of 10 °C/min. The tensile strength of the membranes was measured by using the Universal Tensile Machine (UTM) (Zwick/Roell Z100) at 100% humidity and room temperature in comparison to Nafion[®] NR-211 by leaving the UTM samples in water, and performing the test right after. Finally, a membrane with the highest ionic conductivity was selected for fuel cell performance, and it was stacked with commercial Pt electrodes with 0.5 mg/cm² loading. Current-scan test was performed by Scribner 850e fuel cell test bench at 60°C and 80%RH.

2.3. Results and discussion

The copolymerization of SSS monomer from PVDF powder was performed through a single-step radiation induced graft copolymerization. Different solution systems based on water and alcohol mixture were studied and no significant grafting could be observed. The aqueous DMSO solution was considered a suitable candidate for polymerization, since DMSO is totally water miscible, and also PVDF and SSS are both miscible in DMSO. Therefore, by adding water to DMSO, it is possible to control the solvent up-take by PVDF powder in such a way that SSS monomer could gain access to the active sites of PVDF polymer. Additionally, in literature it was shown that the presence of water in the polymerization solution plays a positive role in the graft level both for hydrophobic and hydrophilic monomers [153]. Environmental concerns and health hazards of other similar solvents such as DMF also motivated us to consider DMSO as the key solvent for polymerization.

Although the solution did not totally dissolve the PVDF polymer, during the filtration and washing of PVDF-g-PSSS, it was observed that a precipitation step is required to prevent coagulation of grafted polymer by means of phase separation. Consequently, acetone was introduced to the solution as a spacer and anti-solvent for SSS monomer and homopolymer in the

solution. Later on, methanol was introduced to the solution to precipitate PVDF-g-PSSS, and finally the resulted system was washed in 60°C water to remove solvents, homopolymers and unreacted monomers.

In the membrane casting process, PVDF-g-PSSS copolymer was dissolved in DMSO with 15% wt. ratio at 105°C in order to remove the absorbed water. The copolymer solution was cast on glass plate by means of the tape casting technique. Due to the high boiling point of DMSO, the PVDF-g-PSSS and DMSO solution is intrinsically capable of absorbing water vapour from the environment to induce phase separation of polymer. This behavior led to benefiting from VIPS to form a highly porous structure of cast membranes by leaving the samples after tape casting in 60%RH air until they formed an opaque appearance. During the film preparation it was observed that the mechanical properties of the films highly depended on the solvent evaporation temperature that is very similar to the pristine PVDF casting systems. To the best of our knowledge, a new solution casting system was developed in such a way that the evaporation temperature of the solution was kept above the melting point of PVDF but below the boiling point of DMSO. In this method the resulted films benefited from the mechanical properties of the melt casting membranes. The resulted film was separated by using a water and methanol solution since the water itself can be absorbed too much by the membrane and causing stress and deformation in the membrane. Later on, the membrane was kept for 24 hours at 60°C to remove the remained solvents, and activated in 1M HCl aqueous solution for 12 hours. The PVDF-g-PSSA membranes were washed several times before drying.

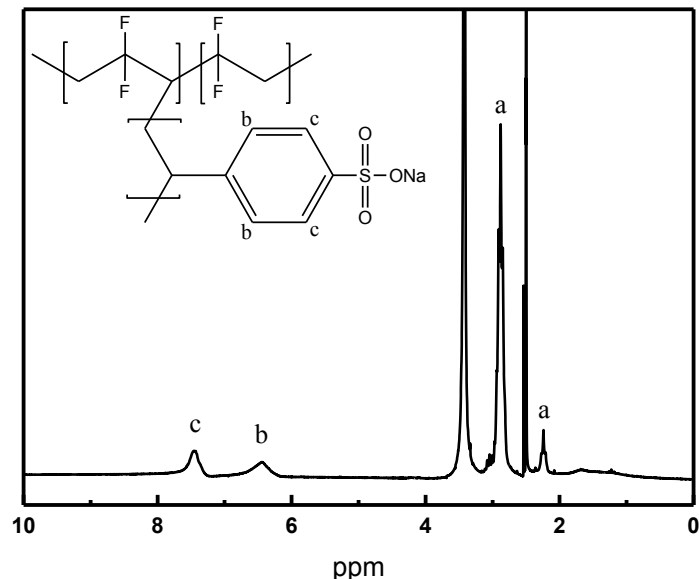


Figure 2. 1. ¹H-NMR result of PVDF-g-PSSS, “a” peaks belong to PVDF, and “b” and “c” peaks belong to SSS.

2.3.1. Graft level

The covalent bonding between PVDF and PSSS was verified by ¹H-NMR at peaks 6.5 and 7.5 ppm (Figure 2.1) [154][155]. By knowing the molar ratio of SSS monomer, the graft level was calculated with respect to PVDF. Grafting reactions with different combinations of water content and 0.2M H₂SO₄ concentration were performed in order to determine the optimum graft condition. It was noticed that the maximum graft level occurs at 20% v% water in the solution (Table 2.1). Moreover, it was observed that H₂SO₄ prevents the polymer damage by reducing the pH level of the copolymerization solution.

Table 2. 1. The effect of water content in the polymerization solution to graft level.

| Water Content (v/v%) | 10% | 20% | 30% | 40% | 50% |
|----------------------|-----|-----|-----|-----|-----|
| Graft Level (wt%) | 30% | 35% | 30% | 25% | 4% |

By varying the grafting time, it was indicated that grafting occurs very fast at the beginning of the reaction, but further increase in the experiment duration does not have a significant effect on the graft level (Figure 2.2). It was demonstrated that grafting continues up to one hour and after one hour the grafting process stops at around 35% wt%. This behavior can occur due to the solution polarity and solutes concentration, or radical transfer to the homopolymers which is very common in the other irradiation grafting systems [126, 156, 157]. In addition, some other behavior might be associated with the grafting behavior of SSS due to forming an amphiphilic polymer structure such as the gel effect [158].

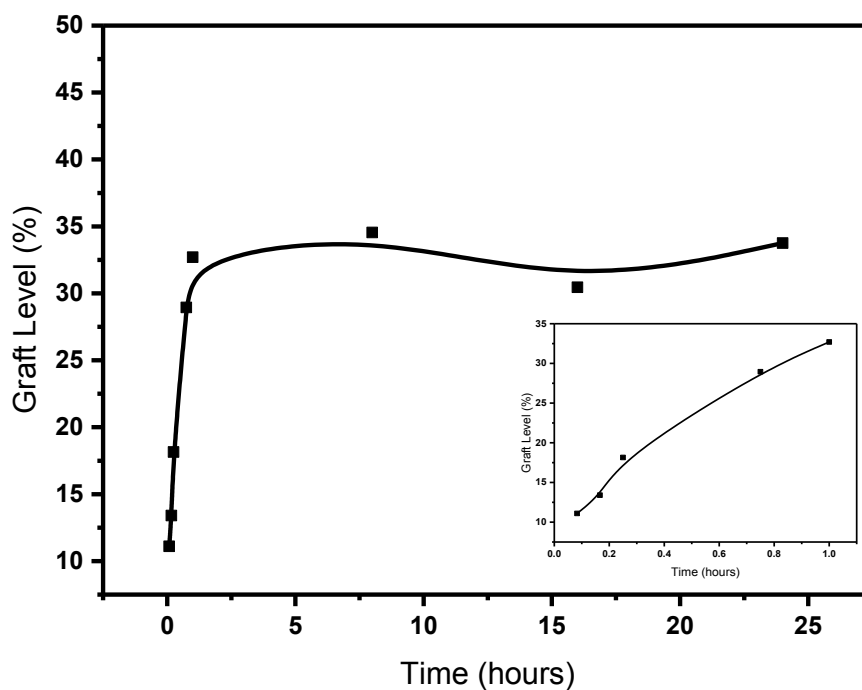


Figure 2. 2. Graft level of PVDF-g-PSSS with respect to reaction time.

2.3.2. Water up-take

The membranes prepared using the VIPS method with varying graft levels after the casting process were activated, dried and hydrated again in order to measure their water up-take (Figure 2.3). The membranes with graft levels below 18% did not show any significant water up-take. As

the graft level increases, there is a sharp increase in water up-take up to 50%. Later on, although the graft level increases, the water up-take increases at a much slower rate. This behavior can be contributed to the interconnection of nano-voids inside the membrane which become less pronounced as the graft level increases.

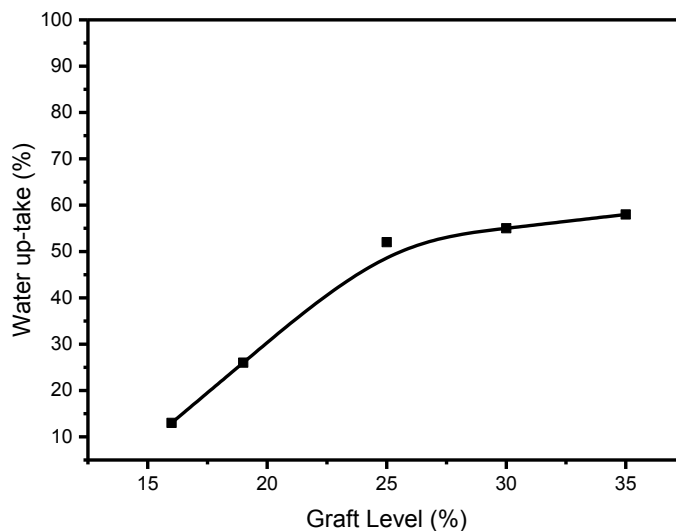


Figure 2. 3. The relation between graft level and water up-take of membranes prepared by VIPS method.

2.3.3. Proton conductivity

Comparing the proton conductivity of PVDF-g-PSSA membranes at different graft levels reveals that there is not a considerable conductivity below 18% grafting degree (Figure 2.4). Similar to Nafion[®], as the amount of water increases, the conductivity is enhanced, too. The water channels and clusters grow and the amount of available free liquid water rises, as well. This results in an enhancement of Grotthuss-type hopping, which increases the proton transport [16]. In order to have a high conductivity, these water clusters must be interconnected to facilitate the Grotthuss-type conductivity. In order to shape the water channels, the interconnection of water clusters occurs at graft levels above 16%, and at room temperature for the current system.

The scanning electron microscopy of membranes revealed the formation of interconnected nano-spheres of grafted polymer (Figure 2.5). Since the graft polymerization is not a controlled

polymerization, therefore it is expected that the graft polymerization has a wide polydispersity index (PDI). As a result, the formation of nano-spheres can be explained in such a way that the penetration of water vapour in polymer solution system causes the less grafted PVDF branches (which are more hydrophobic) to first form the core of particles roughly around 200 nm, and the more grafted polymer backbones (which are less hydrophobic) to form the shell and the interconnections between particles.

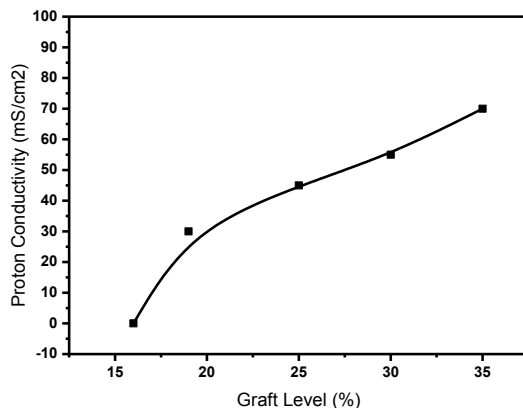


Figure 2. 4. Proton conductivity of the membranes prepared by tape casting and mold casting.

This phenomenon results in the formation of ionic channels and their efficient interconnections. The formation of ionic domains through modifying the architecture of water channels is the reason for the increase in ionic conduction [159].

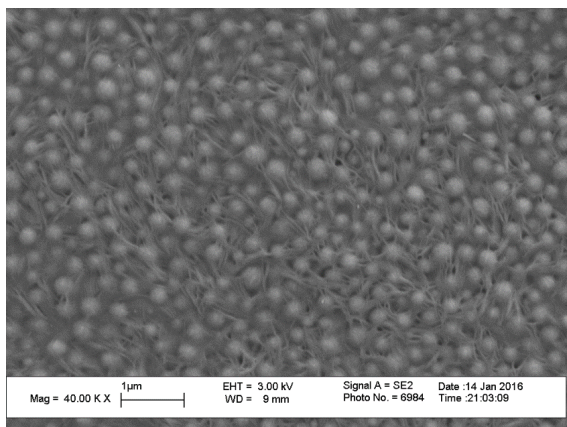


Figure 2. 5. Scanning electron microscopy imaging of sub-micron structure of PVDF-g-PSSS membrane with 35% graft level.

2.3.4. Thermogravimetric analysis

Thermal analysis of the membranes was performed up to 800°C with the rate of 10 °C/min to evaluate the membrane properties (Figure 2.6), and these results are very similar to PSSS and PSSA thermogravimetric results [160]. Up to 100°C PVDF-*g*-PSSS, and its acidic form (PVDF-*g*-PSSA), and Nafion[®] NR-211 all show a significant loss which is mostly due to the evaporation of water in their hydrophilic structure. From 100°C to 250°C all the membranes share an insignificant weight loss, but above 250°C the rate of degradation starts to increase with the slowest rate belonging to PVDF-*g*-PSSS. Since during membrane preparation, the activation of membranes comes after film casting procedure, therefore PVDF-*g*-PSSS is still in salt form, and it has the least susceptibility toward thermal degradation during the evaporation of solvent at 180°C.

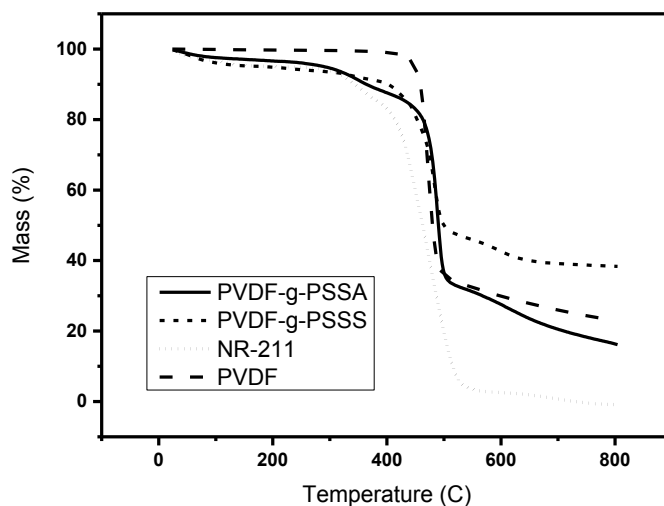


Figure 2. 6. Thermogravimetric analysis of PVDF-*g*-PSSA compared to pristine PVDF, PVDF-*g*-PSSS and Nafion[®] NR-211.

2.3.5. Mechanical properties

The tensile strength test was performed for the determination of the mechanical properties of membranes at 100%RH (Figure 2.7). As it was observed, the PDVF-*g*-PSSA radiation grafted membranes at 100%RH exhibit a higher plasticity than Nafion[®] NR-211 at 30% graft level. In the graph, as the graft level increases the mechanical properties reduce up to 20% graft level.

Due to a higher water uptake, membranes with a 20% more graft level show more elongation. The increment in grafting degree after 20% slowly reduces membrane stiffness and increases its elongation. In addition, we observed that the presence of water in the casting solution (during VIPS process) affects both mechanical properties and membrane porosity with respect to solvent evaporation temperature. The membranes which were prepared below 100°C essentially have very weak mechanical properties, but possess instead a very high proton conductivity up to 200 (mS/cm²). As the temperature rises, the phase separation becomes less pronounced, and the polymer chains become orderly and oriented, resulting in higher mechanical properties and less proton conductivity up to the melting point of PVDF.

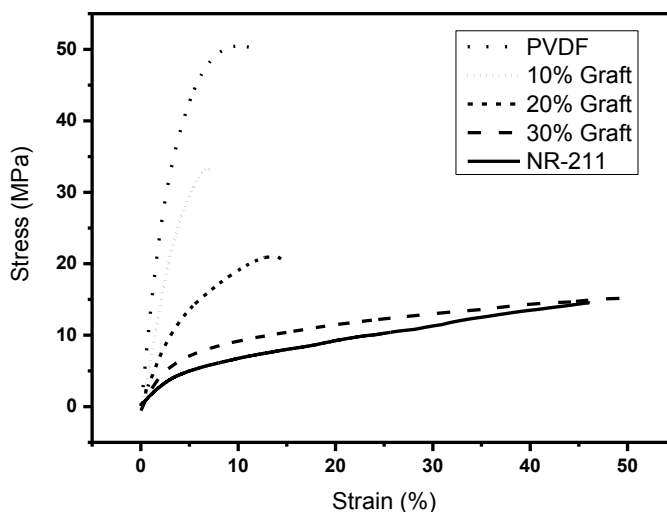


Figure 2. 7. The universal tensile stress results of fully humidified PVDF-g-PSSA membrane with different graft levels.

2.3.6. Fuel Cell performance

The fuel cell performance of 35% grafted PVDF-g-PSSA membrane was measured at 60° and 80%RH under H₂/O₂ feed gases (Figure 2.8). The commercial electrodes were used without any further modification. The cell demonstrated an open circuit voltage (OCV) of 0.97(V), then after applying the load it was reduced to 0.8(V) due to activation losses. Interestingly, the current-voltage curves followed almost a straight line up to 0.01(V) which indicates the absence of diffusion losses at high current densities at three phase boundary. The maximum power density

of 250 (mW/cm^2) was achieved at 0.4(V) and 650 (mA/cm^2). Although the PVDF-g-PSSA membrane was prepared for the first time, compared to Nafion[®] NR-211 the prepared membrane could show relatively good results. Also like any other styrene sulfonic acid based membrane, the PVDF-g-PSSA membrane also demonstrated reduction in performance during continuous operation which is due to losing the sulfonic acid groups by means of hydroxyl radicals [140].

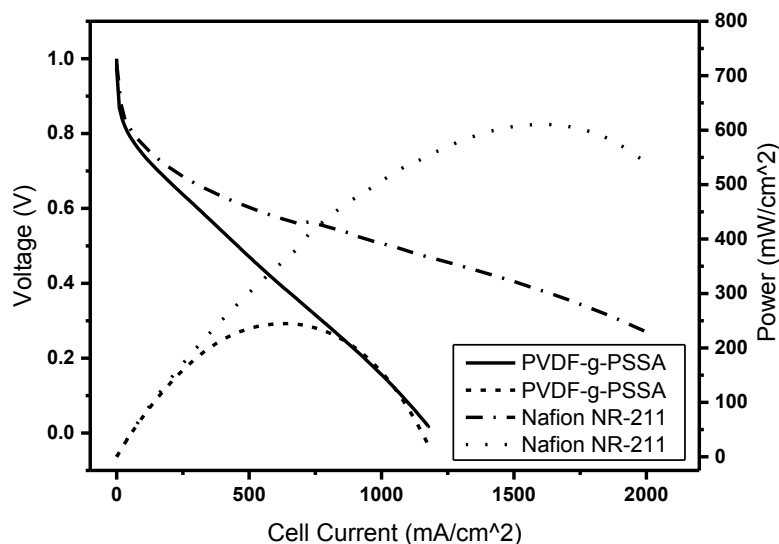


Figure 2. 8. Current-voltage and current-power of fuel cell performance of 35% grafted PVDF-g-PSSA at 60°C and 80%RH vs. Nafion[®] NR-211 at 80°C and 60%RH.

2.4. Conclusions

A facile method to prepare a sulfonated proton exchange membrane with nano-porosity was successfully developed and characterized for the first time in the literature. The grafting process of PVDF-g-PSSS was verified by means of H-NMR, and further membrane characterization was carried out for graft level, ionic conductivity, thermogravimetric analysis, and measuring mechanical tensile strength. By means of the VIPS method, the developed amphiphilic grafted polymer membranes demonstrated conductivities comparable to Nafion[®]. Additionally, a new solution casting method was used to retain the mechanical properties of membranes as close to the melt casting process as possible. In the actual fuel cell environment, the PVDF-g-PSSA membranes could present fuel cell characteristics relatively close to Nafion[®] NR-211.

3. CROSS-LINKED PROTON EXCHANGE MEMBRANES BY RADIATION INDUCED GRAFTING OF 4-VINYLPYRIDINE AND DIVINYLBENZENE FROM POLY(ETHYLENE-CO-TETRAFLUOROETHYLENE) FILMS

Research Objectives

The classical hydrogen fuel cell needs to operate below 80°C because of the degradation of Nafion[®] membrane above this temperature. Low temperature operation of fuel cell results in CO poisoning of electrodes, low energy density, and water formation in the gas manifolds. Therefore, in this project an acid-base type of membrane for fuel cell applications between 80°C to 120°C by means of radiation graft polymerization of cross-linked poly(4-vinylpyridine-co-divinylbenzene) from poly(ethylene tetrafluoroethylene) films with consequence phosphoric acid doping is proposed for the first time. Since during graft polymerization process the mechanical properties of films usually decrease, the introduction of cross-linker (divinylbenzene) in the grafted polymer matrix is expected to improve the mechanical properties of grafted membranes. Additionally, in this study the influence of cross-linking over polymerization kinetics, mechanical properties, acid up-take, proton conductivity and fuel cell performance will also be studied.

3.1. Introduction

Energy supply plays a crucial role in economic, environmental and social development. A sustainable society requires energy resources which are economically affordable, environmentally friendly, and as little as possible relying on depletable or foreign resources. Fuel cell technology, among other types of renewable energy resources, has already proven its capabilities. Although this technology is utilized in many different sectors, yet there are possibilities to improve performance and efficiency of fuel cell systems. One of the promising areas of research in this field is high temperature polymer electrolyte membrane fuel cells (HT-PEMFC) operating at temperatures above 100°C. HT-PEMFC is very desirable due to improved electrode kinetics, enhanced ionic conductivity and reduced humidification. The performance of low temperature (LT) PEMFC normally suffers from catalyst poisoning by carbon monoxide [161], water flooding problem in the cell [162], and poor performance for combined heat and power (CHP) systems. Therefore, increasing the operating temperature of PEMFC has recently attracted the attention of researchers [26].

Polymeric proton exchange membranes (PEM), due to their acidic groups that are attached to their polymer backbone, are capable of proton conduction through nano-sized water channels. Membranes with perfluorinated sulfonic acids such as Nafion[®] manufactured by DuPont are the most widely used PEM for fuel cell applications due to their high proton conductivity and stability under harsh conditions. For operating temperatures above 100°C, the relative humidity of PEM decreases and this leads to a reduction or loss of proton conductivity in the PEM [163, 164]. In addition, at elevated temperatures the membrane degradation is facilitated, which consequently results in the loss of ionic conductivity [165].

Phosphoric acid doped polymer membranes are considered a suitable candidate for PEM applications. In this method a polymer membrane with basic pendant groups such as poly(benzimidazole) (PBI) is soaked in phosphoric acid [166]. The attraction between phosphoric acid and the basic sites of the membrane results in the immobilization of phosphoric acid in the polymer matrix. Besides PBI, other types of basic polymers such as sulfopropylated poly(benzimidazole) [167], polybenzimidazole [168], phosphonated fully aromatic polyethers [169], sulfonated polybenzimidazoles [170] were also developed for HT-PEMFC.

Radiation induced graft polymerization (RIGP) is a *grafting-from* type of polymerization in which active sites are generated by radiation. Recently, in order to provide a high acid doped acid-base polymer membrane system RIGP was used to graft polymerize basic monomers from poly(ethene-co-tetrafluoroethene) (ETFE) films. The grafting of 4-vinylpyridine (4VP) from ETFE films has so far provided excellent fuel cell performance for HT-PEMFC applications [132, 133, 171-173]. During the radiation and grafting process the ETFE film partially loses its mechanical strength [117]. Therefore, Nasef et al. studied the effect of triallyl-cyanurate (TAC) on ETFE-g-P4VP, and they observed an improvement in the mechanical properties of cross-linked membranes [174]. Additionally, they observed a higher phosphoric acid up-take during the doping process which, in turn, led to a higher ionic conductivity of grafted membranes. In another study Chen et al. studied the effect of different cross-linkers on the properties of ETFE membranes, and he concluded that divinylbenzene (DVB) shows better chemical stability compared to the other cases in their study [175].

In this work, we studied the effect of divinylbenzene (DVB) cross-linker on the physicochemical properties of irradiation graft polymerization of 4-vinylpyridine and poly(ethylene-co-tetrafluoroethylene) (ETFE) films for HT-PEMFC application. The process commences with cutting ETFE films in desired dimensions, and later on irradiating them with gamma rays by using a suitable dosage to generate radicals on the polymer backbone. Afterwards, graft polymerization proceeds through an oxygen free solution of monomer(s) and suitable solvent(s) by immersing the irradiated film. The resulted film from polymerization is washed, dried and doped with phosphoric acid.

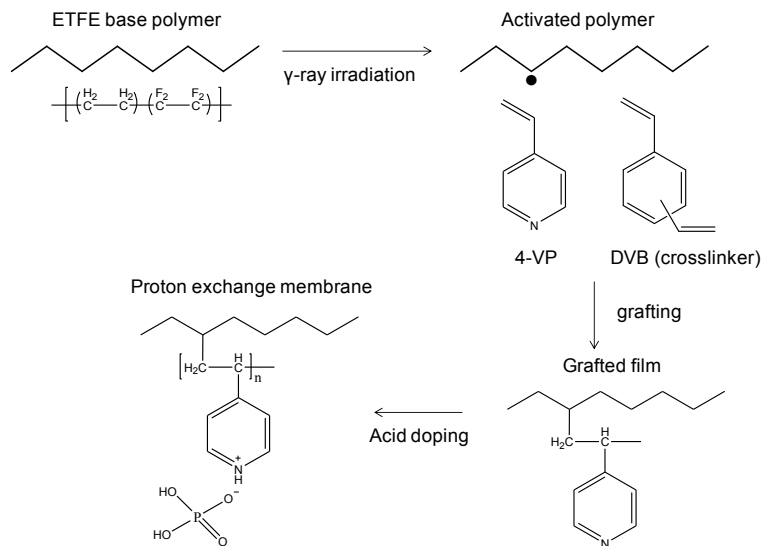


Figure 3. 1. Mechanism of preparation of cross-linked phosphoric acid doped poly(4VP) grafted ETFE membrane.

The conjugation of phosphoric acid with nitrogen in a pyridine ring provides a suitable condition for proton conduction at elevated temperatures, while ETFE backbone provides the required mechanical stability for the membrane. In order to further improve the mechanical properties of membrane, DVB is introduced during the polymerization to strengthen its mechanical properties due to the cross-linked rigid network (Figure 3.1).

3.2. Experimental

3.2.1. Materials

The base polymer ETFE with 25 micron thickness was purchased (Nowoflon ET-6235) from Nowofol GmbH (Siegendorf, Germany). The reagents isopropanol (IPA), tetrahydrofuran (THF), 4-vinylpyridine (4VP), divinylbenzene (DVB), phosphoric acid (PA) were all purchased from Sigma Aldrich, and were used without any further purification.

3.2.2. Membrane preparation

The ETFE films were first cut and then washed with ethanol, and later on dried overnight. The films were afterwards weighted, and packed in small polyethylene plastic bags. The irradiation process was carried out in γ -rays via ^{60}Co source at 50 kGy total irradiation dose at room temperature. After irradiation, the ETFE films were kept in deep freeze. The polymerization performed in a 36 (ml) polymerization solution of IPA, THF and 4VP with volumetric ration of 1:2:3 in a cylindrical reactor. The DVB was added to the solution with different volumetric ratios with respect to 4-VP concentration ranging from 0% to 2%. The prepared solution was degassed with nitrogen for 30 minutes, and then left at 60°C in different reaction times. After grafting the process, the resulted polymer was washed in a 1:1 volumetric solution of IPA and THF overnight, and dried in the oven for 24 hours at 60°C. The grafted ETFE-g-PVP membranes were later on acid doped by soaking the membranes in PA with 85% concentration for 20 hours. After acid doping, the excess acid was wiped from the surface of membranes with tissue paper and without any washing.

3.2.3. Characterization of membranes

To measure the graft level, the radiation grafted copolymers were left in the room conditions after drying in the oven in order to lose their electrostatic charge during drying. Later, the graft level was measured by comparing the weight increase of the membranes with respect to their original weight. The equation for graft level is as follows (Equation 3.1):

$$\text{Graft level} = \frac{W_g - W_o}{W_o} \times 100 \quad (3.1)$$

where W_g and W_o are the weights of grafted and original ETFE films, respectively. The phosphoric acid up-take of membranes was measured by comparing the weight of fully acid doped membranes right after the doping process with respect to their grafted weight. The PA up-take was calculated by (Equation 3.2):

$$\text{Phosphoric acid uptake} = \frac{W_d - W_g}{W_g} \times 100 \quad (3.2)$$

where W_d and W_g are the weights of acid doped and grafted membranes, respectively. In addition, the proton conductivity of these membranes was measured at different temperatures and relative humidities under N_2 by means of Becktech 4-point probe conductivity device and Scribner 850e fuel cell test station. The tensile strength of the membranes was measured by Universal Tensile Machine (UTM) (Zwick/Roell Z100) at 60%RH and room temperature. The effect of DVB on the surface properties of grafted membranes was also investigated by measuring the contact angle. Scanning electron microscopy (SEM) imaging and energy-dispersive X-ray spectroscopy (XEDS) mapping of membranes were performed by Zeiss Gemini electron microscope. Additionally, membranes with DVB and without DVB were selected for fuel cell performance, and they were stacked with commercial PTFE treated electrodes with 0.5 mg/cm² Pt loading. Finally, the current-scan test was carried out by Scribner 850e fuel cell test bench at 50%RH and varying temperatures.

3.3. Results and discussion

3.3.1. The effect of reaction time on graft level

The polymerization reaction was performed at 60°C by immersing the cylindrical reactor in a silicon oil bath after placing the radiated film in the solution and purging nitrogen. Different reactions by varying reaction time for 0% DVB concentration and 1% DVB concentration in 50% monomer concentration solution of 1:2 IPA-THF solution were also performed. After washing grafted films with IPA-THF solution overnight, the membranes were dried and weighted. The graft levels for the obtained membranes for durations from 1 to 6 hours are plotted in (Figure 3.2). Quite similar to the other free radical graft polymerizations, up to one hour the reaction rate is very fast, but as the reaction proceeds the rate of reaction slows down [116, 118, 123]. The reason for this phenomenon is the radical transfer from grafting sites to the solution. This effect is very perceivable especially in the presence of DVB in such a way that after 6 hours the polymerization solution totally turns into a gel. The main reason for considering the IPA-

THF binary solution was due to the fact that this system is capable of forming a transparent mixture of polymerization elements without any phase separation.

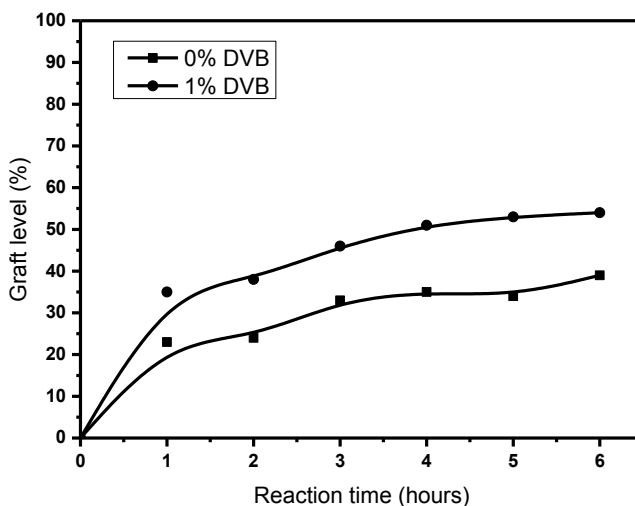


Figure 3. 2. The graft level of ETFE-g-PVP films with 0%DVB and 1%DVB at 60°C, 50 kGy and varying reaction time.

3.3.2. The Effect of DVB concentration on graft level

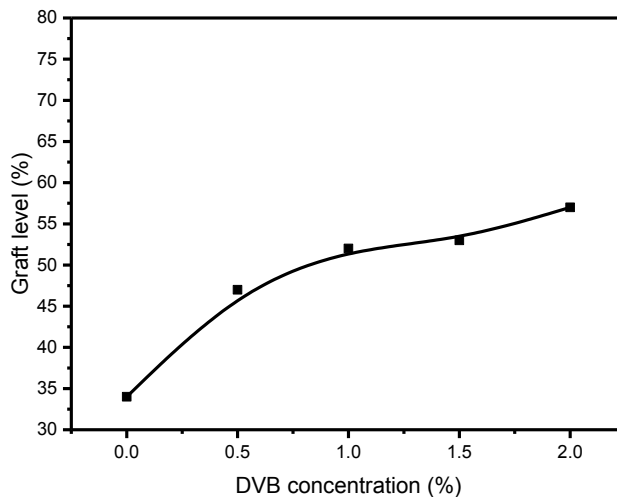


Figure 3. 3. The effect of DVB concentration on graft level of 50 kGy ETFE films at 60°C and 4 hours grafting time.

Comparing the effect of DVB on graft level of membranes, it is evident that DVB addition to the monomer could increase the graft level by more than 40% (Figure 3.3). This effect can be

explained by fixation of growing chains and preventing the radical termination [118, 175]. The graft level increases considerably for 0.5% and 1% samples, and for the samples with higher DVB concentration the increase is negligible.

3.3.3. The effect of DVB on phosphoric acid up-take

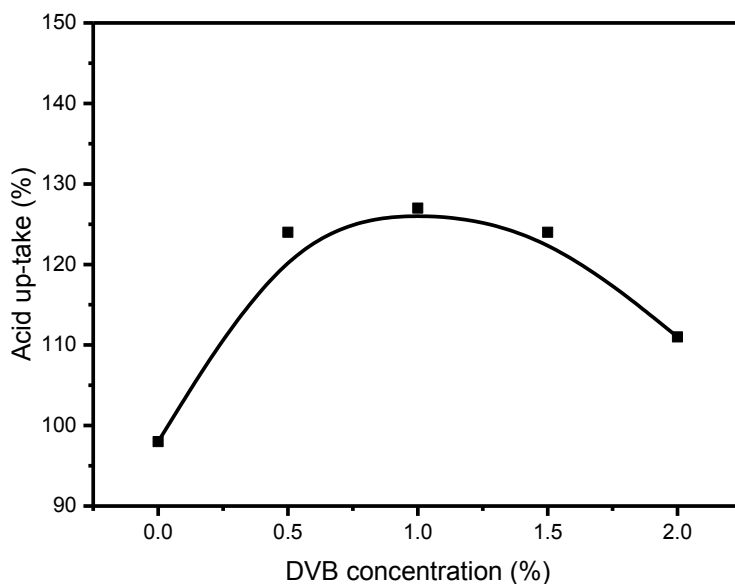


Figure 3. 4. The effect of DVB concentration on the phosphoric acid up-take during doping process.

Phosphoric acid doping was performed by immersing the grafted films in 85% phosphoric acid for 20 hours. Later the extra acid of the membranes was wiped with tissue paper, and immediately weighted. The results of acid doping indicate that as the graft level increases, the acid up-take also increases. In contrast, introducing the cross-linker has a negative effect on the acid up-take by limiting the polymer matrix from expansion (Figure 3.4). Increasing the DVB amount up to 1% maximizes acid up-take, and the further increase in DVB results in lower acid up-take despite the fact that the graft level increases.

3.3.4. The effect of DVB on phosphoric acid loss

Samples of 0% and 1% DVB were selected and washed with water in order to determine the effect of DVB on the internal film structure. The SEM images of membranes demonstrate the fact that in case of 0% DVB the grafted polymer is not interconnected, and although it is able to take more acid compared to the cross-linked membranes, washing will lead to the formation of voids inside the membrane (**Figure 3.5**). In contrast, the graft structure of 1%DVB membranes forms interconnected polymer networks which resist against acid loss due to washing.

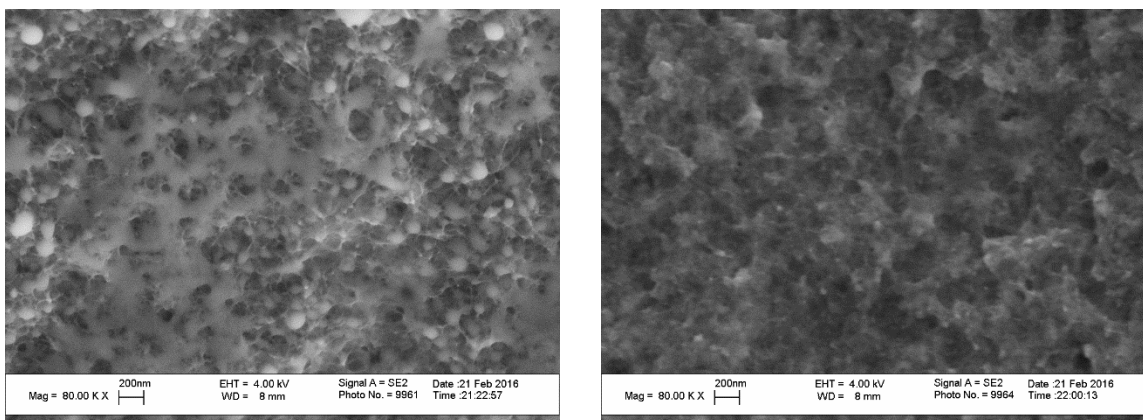


Figure 3. 5. Scanning electron microscope image of grafted ETFE films: left) 0%DVB grafted film right) 1%DVB grafted film.

The further investigation of these phenomena continued by selecting two membranes of 0% and 1% DVB, but with the same graft level. This time the effect of acid up-take was investigated by measuring the acid amount with respect to the absolute amount of grafted polymer (Figure 3.6). Additionally, two membranes of 0% and 1% DVB which had the same amount of doped acid were selected. The effect of washing for the membranes with the same graft level showed that the membrane with 1% DVB can take almost 50% less acid compared to the non-cross-linked membrane. However, after washing the membranes with the same acid amount, it was observed that the membrane with 0% DVB lost more than 50% of its acid, while the 1% DVB membrane only lost less than 20% of its acid.

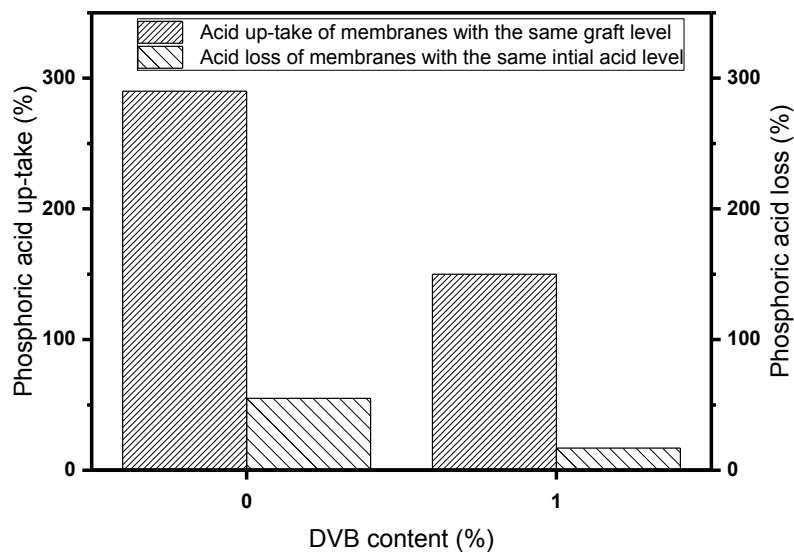


Figure 3. 6. The effect of DVB on acid up-take and acid loss of grafted membranes with the same initial conditions.

The contact angle of acid doped membranes showed the underlying mechanism of resistance to acid loss in cross-linked samples (Figure 3.7). The membrane with 0% DVB almost did not show any hydrophobicity towards water. Surprisingly, the 1% DVB membrane showed a contact angle more than 60°. This behavior can be explained through the *lotusutos effect* due to the formation of nan-structured cross-linked acid pores in the membrane [176].

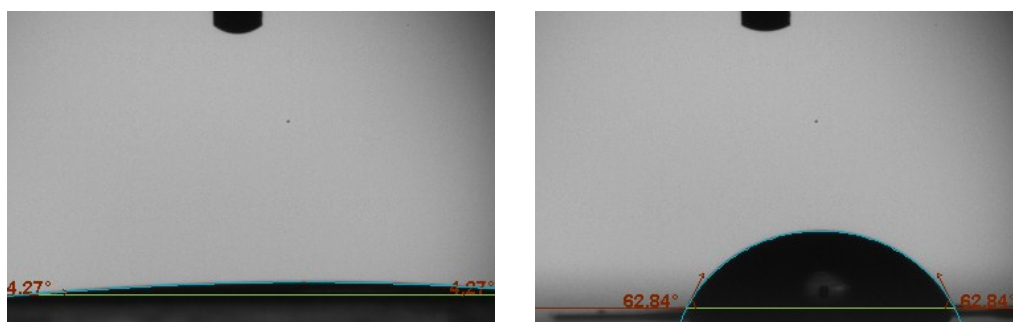


Figure 3. 7. The effect of cross-linking on contact angle of acid doped membranes: left) 0% DVB mebrane, right) 1% DVB membrane.

3.3.5. The effect of DVB on mechanical properties of membranes

The tensile test was carried out for the acid doped synthesized membranes with 1:10 aspect ratio at 100 mm/min elongation rate. The introduction of DVB up to 0.5% did not show a significant contribution to the mechanical properties of membranes. At 1% DVB concentration the membrane could show the highest elongation among the other samples because of the formation of an interconnected network of grafted polymers. Although further increasing DVB concentration led to increasing the strength of membranes, this increase also caused the decrease of the elongation (Figure 3.8). Moreover, the physical appearance of membranes also depends on crosslinking in such a way that after acid doping the 0% DVB membranes show a white appearance due the interference of membrane voids with visible light, and consequently scattering the light. However, the cross-linked membranes could maintain their transparency after acid doping.

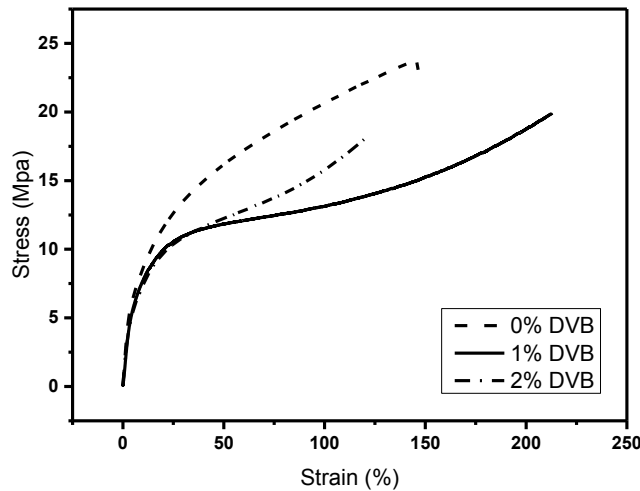


Figure 3. 8. The tensile test results for acid doped membranes with 0%, 1% and 2% DVB content.

3.3.6. Ionic conductivity of grafted membranes

The ionic conductivity of grafted membranes was measured by means of a 4-probe conductivity cell placed in a special apparatus for controlling temperature and relative humidity of membranes during the measurements. Three membranes were studied, 0% DVB content with 30% graft level, 1% DVB with same graft level as 0% DVB membrane, and 1% DVB with 50% graft level.

These membranes were tested at 80°C, 100°C and 120°C and varying relative humidity ranging from 10% to 50% (Figure 3.9). Although the membranes were not washed, the ionic conductivity of all membranes changed drastically by changing the RH. Additionally, all of the conductivity values increased as the operating temperature rose. The maximum ionic conductivity of 75 mS/cm² belonged to 1% DVB membrane with 50% graft level. Interestingly the 0% DVB could also reach a 60 mS/cm² conductivity, which is due to the high phosphoric acid up-take.

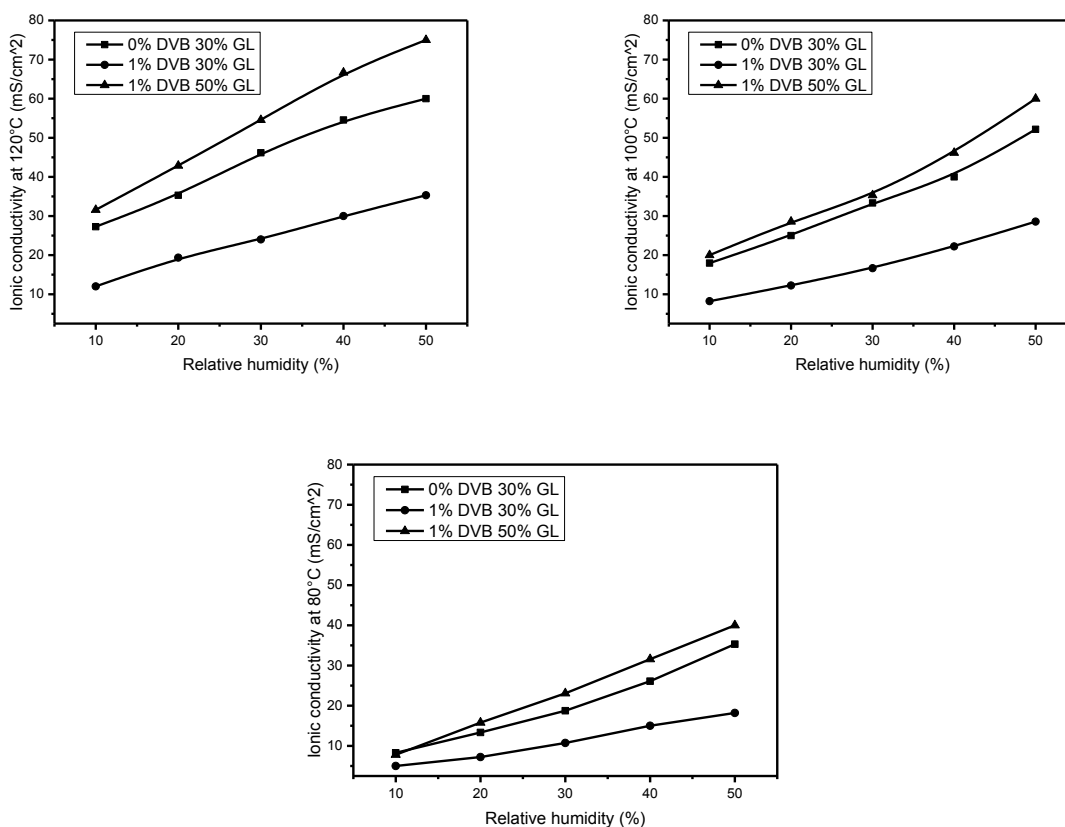


Figure 3. 9. The proton conductivity of ETFE-g-PVP membranes at different relative humidity and temperature.

3.3.7. Fuel cell performance of ETFE-g-PVP membranes

The fuel cell performance of membranes with 0% DVB and 30% graft level, and 1% DVB and 50% graft level was measured at 1 atmosphere gauge pressure and 50%RH at different temperatures (Figure 3.10). Surprisingly, the fuel cell performance of cross-linked membrane under all conditions was much better than the non-cross-linked membrane despite their similar

proton conductivities. This is because of the fact that the phosphoric acid inside the membrane, due to interaction of phosphoric acid with gas diffusion layer, interferes with the three phase boundary mechanism of electrodes [177]. Therefore, it can be speculated that the reason for the improvement of cell performance is the capability of cross-linked membrane which withholds phosphoric acid inside the membrane.

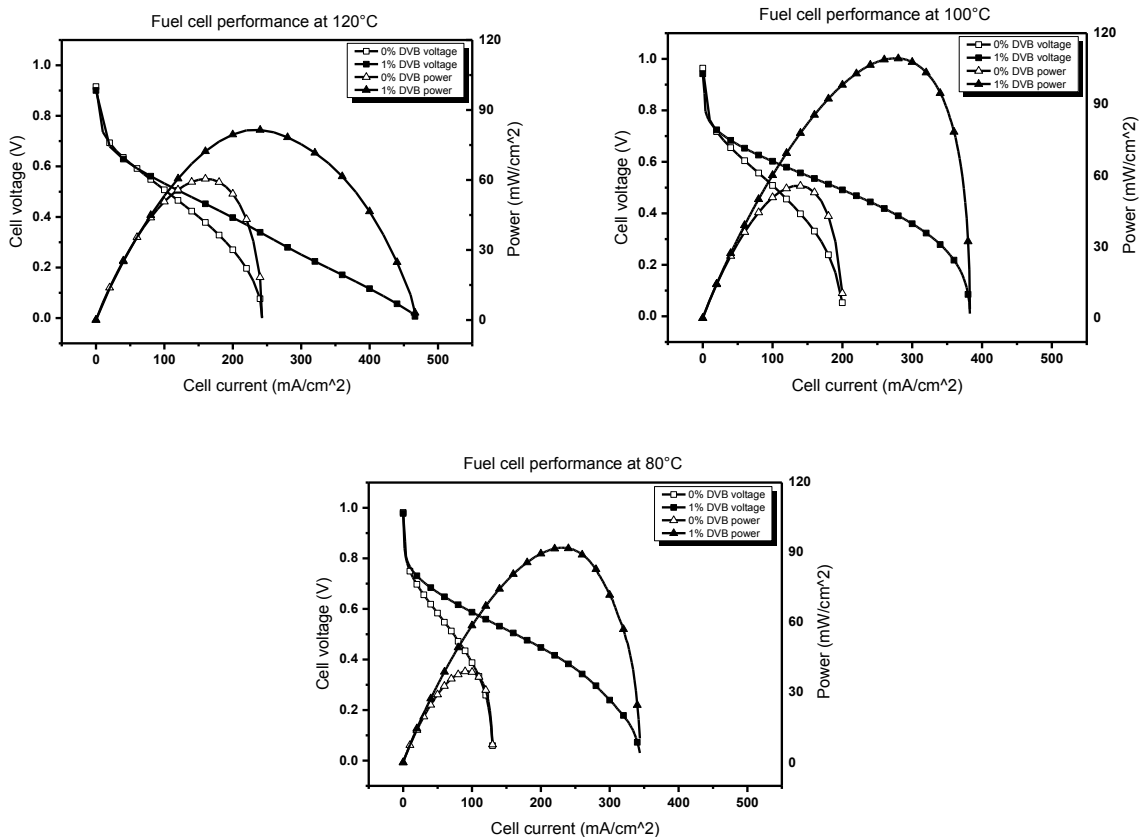


Figure 3. 10. Fuel cell performance of ETFE-g-PVP at 50%RH, 1 atm and different temperatures.

3.4. Conclusion

Cross-linked ETFE based membranes were synthesized via radiation induced grafting of 4VP with varying DVB concentration successfully, and were further modified by means of subsequent doping with phosphoric acid. The obtained membranes were characterized for graft level, acid up-take, mechanical properties and fuel cell performance. It was observed that the introduction of 1% DVB to the structure of grafted polymer optimizes ETFE-g-PVP membranes

in terms of mechanical properties, proton conductivity, and power output. It is speculated that modifying the nano-structure of cross-linked membrane is the reason for its hydrophobicity which eventually led to a more efficient formation of the three-phase boundary between membrane, electrode, and reactant gases.

REFERENCES

1. *ALoysio luigi galvani (1737-1798) discoverer of animal electricity*. JAMA, 1967. **201**(8): p. 626-627.
2. Simon, P. and Y. Gogotsi, *Capacitive Energy Storage in Nanostructured Carbon-Electrolyte Systems*. Accounts of Chemical Research, 2013. **46**(5): p. 1094-1103.
3. Cecchini, R. and G. Pelosi, *Alessandro Volta and his battery*. Antennas and Propagation Magazine, IEEE, 1992. **34**(2): p. 30-37.
4. Mills, A.A., *Early Voltaic Batteries: an Evaluation in Modern Units and Application to the Work of Davy and Faraday*. Annals of Science, 2003. **60**(4): p. 373-398.
5. Williams, L.P., *Michael Faraday's chemical notebook: portrait of the scientist as a young man*. Physics Education, 1991. **26**(5): p. 278.
6. https://en.wikipedia.org/wiki/Fuel_cell.
7. Perry, M.L. and T.F. Fuller, *A Historical Perspective of Fuel Cell Technology in the 20th Century*. Journal of The Electrochemical Society, 2002. **149**(7): p. S59-S67.
8. Badwal, S.P.S., S.S. Giddey, C. Munnings, A.I. Bhatt, and A.F. Hollenkamp, *Emerging electrochemical energy conversion and storage technologies*. Frontiers in Chemistry, 2014. **2**.
9. Pohl, E., P. Meier, M. Maximini, and J.v. Schloß, *Primary energy savings of a modular combined heat and power plant based on high temperature proton exchange membrane fuel cells*. Applied Thermal Engineering, 2016. **104**: p. 54-63.
10. Buonomano, A., F. Calise, M.D. d'Accadia, A. Palombo, and M. Vicidomini, *Hybrid solid oxide fuel cells-gas turbine systems for combined heat and power: A review*. Applied Energy, 2015. **156**: p. 32-85.
11. Li, Q.S., J. Gong, S.K. Peng, S.F. Lu, P.C. Sui, N. Djilali, and Y. Xiang, *Theoretical design strategies of bipolar membrane fuel cell with enhanced self-humidification behavior*. Journal of Power Sources, 2016. **307**: p. 358-367.
12. Peng, S.K., X. Xu, S.F. Lu, P.C. Sui, N. Djilali, and Y. Xiang, *A self-humidifying acidic-alkaline bipolar membrane fuel cell*. Journal of Power Sources, 2015. **299**: p. 273-279.
13. Shaegh, S.A.M., N.T. Nguyen, and S.H. Chan, *A review on membraneless laminar flow-based fuel cells*. International Journal of Hydrogen Energy, 2011. **36**(9): p. 5675-5694.
14. Rahimnejad, M., A. Adhami, S. Darvari, A. Zirepour, and S.E. Oh, *Microbial fuel cell as new technology for bioelectricity generation: A review*. Alexandria Engineering Journal, 2015. **54**(3): p. 745-756.
15. Wang, H.M., J.D. Park, and Z.J. Ren, *Practical Energy Harvesting for Microbial Fuel Cells: A Review*. Environmental Science & Technology, 2015. **49**(6): p. 3267-3277.
16. Kraysberg, A. and Y. Ein-Eli, *Review of Advanced Materials for Proton Exchange Membrane Fuel Cells*. Energy & Fuels, 2014. **28**(12): p. 7303-7330.
17. Zhang, H.W., D.Z. Chen, Y. Xianze, and S.B. Yin, *Anion-Exchange Membranes for Fuel Cells: Synthesis Strategies, Properties and Perspectives*. Fuel Cells, 2015. **15**(6): p. 761-780.

18. Varcoe, J.R., P. Atanassov, D.R. Dekel, A.M. Herring, M.A. Hickner, P.A. Kohl, A.R. Kucernak, W.E. Mustain, K. Nijmeijer, K. Scott, T.W. Xu, and L. Zhuang, *Anion-exchange membranes in electrochemical energy systems*. Energy & Environmental Science, 2014. **7**(10): p. 3135-3191.
19. Scott, K., C.X. Xu, and X. Wu, *Intermediate temperature proton-conducting membrane electrolytes for fuel cells*. Wiley Interdisciplinary Reviews-Energy and Environment, 2014. **3**(1): p. 24-41.
20. Bidault, F., D.J.L. Brett, P.H. Middleton, and N.P. Brandon, *Review of gas diffusion cathodes for alkaline fuel cells*. Journal of Power Sources, 2009. **187**(1): p. 39-48.
21. Merle, G., M. Wessling, and K. Nijmeijer, *Anion exchange membranes for alkaline fuel cells: A review*. Journal of Membrane Science, 2011. **377**(1-2): p. 1-35.
22. Sammes, N., R. Bove, and K. Stahl, *Phosphoric acid fuel cells: Fundamentals and applications*. Current Opinion in Solid State & Materials Science, 2004. **8**(5): p. 372-378.
23. Neergat, M. and A.K. Shukla, *A high-performance phosphoric acid fuel cell*. Journal of Power Sources, 2001. **102**(1-2): p. 317-321.
24. Bose, S., T. Kuila, X.L.N. Thi, N.H. Kim, K.T. Lau, and J.H. Lee, *Polymer membranes for high temperature proton exchange membrane fuel cell: Recent advances and challenges*. Progress in Polymer Science, 2011. **36**(6): p. 813-843.
25. Chandan, A., M. Hattenberger, A. El-Kharouf, S.F. Du, A. Dhir, V. Self, B.G. Pollet, A. Ingram, and W. Bujalski, *High temperature (HT) polymer electrolyte membrane fuel cells (PEMFC) - A review*. Journal of Power Sources, 2013. **231**: p. 264-278.
26. Liu, Y.F., W. Lehnert, H. Janssen, R.C. Samsun, and D. Stolten, *A review of high-temperature polymer electrolyte membrane fuel-cell (HT-PEMFC)-based auxiliary power units for diesel-powered road vehicles*. Journal of Power Sources, 2016. **311**: p. 91-102.
27. Subianto, S., *Recent advances in polybenzimidazole/phosphoric acid membranes for high-temperature fuel cells*. Polymer International, 2014. **63**(7): p. 1134-1144.
28. Zhang, J.L., Z. Xie, J.J. Zhang, Y.H. Tanga, C.J. Song, T. Navessin, Z.Q. Shi, D.T. Song, H.J. Wang, D.P. Wilkinson, Z.S. Liu, and S. Holdcroft, *High temperature PEM fuel cells*. Journal of Power Sources, 2006. **160**(2): p. 872-891.
29. Ekinci, K.Z., S.U. Ccedil;elik, and A. Bozkurt, *Enhancing the Anhydrous Proton Conductivity of Sulfonated Polysulfone/Polyvinyl Phosphonic Acid Composite Membranes With Hexagonal Boron Nitride*. International Journal of Polymeric Materials and Polymeric Biomaterials, 2015. **64**(13): p. 683-689.
30. Sen, U., H. Usta, O. Acar, M. Citir, A. Canlier, A. Bozkurt, and A. Ata, *Enhancement of Anhydrous Proton Conductivity of Poly(vinylphosphonic acid)-Poly(2,5-benzimidazole) Membranes via In Situ Polymerization*. Macromolecular Chemistry and Physics, 2015. **216**(1): p. 106-112.
31. Sinirlioglu, D., A.E. Muftuoglu, and A. Bozkurt, *Investigation of perfluorinated proton exchange membranes prepared via a facile strategy of chemically combining poly(vinylphosphonic acid) with PVDF by means of poly(glycidyl methacrylate) grafts*. Journal of Polymer Research, 2015. **22**(8).
32. Zitka, J., M. Bleha, J. Schauer, B. Galajdova, M. Paidar, J. Hnat, and K. Bouzek, *Ion exchange membranes based on vinylphosphonic acid-co-acrylonitrile copolymers for fuel cells*. Desalination and Water Treatment, 2015. **56**(12): p. 3167-3173.

33. Berber, M.R., T. Fujigaya, and N. Nakashima, *High-Temperature Polymer Electrolyte Fuel Cell Using Poly(vinylphosphonic acid) as an Electrolyte Shows a Remarkable Durability*. Chemcatchem, 2014. **6**(2): p. 567-571.
34. Berber, M.R., T. Fujigaya, K. Sasaki, and N. Nakashima, *Remarkably Durable High Temperature Polymer Electrolyte Fuel Cell Based on Poly(vinylphosphonic acid)-doped Polybenzimidazole*. Scientific Reports, 2013. **3**.
35. Mohammad, N., A.B. Mohamad, A.A.H. Kadhum, and K.S. Loh, *A review on synthesis and characterization of solid acid materials for fuel cell applications*. Journal of Power Sources, 2016. **322**: p. 77-92.
36. Dupuis, A.C., *Proton exchange membranes for fuel cells operated at medium temperatures: Materials and experimental techniques*. Progress in Materials Science, 2011. **56**(3): p. 289-327.
37. Ikeda, A., D.A. Kitchaev, and S.M. Haile, *Phase behavior and superprotonic conductivity in the Cs_{1-x}Rb_xH₂PO₄ and Cs_{1-x}K_xH₂PO₄ systems*. Journal of Materials Chemistry A, 2014. **2**(1): p. 204-214.
38. Sugahara, T., A. Hayashi, K. Tadanaga, and M. Tatsumisago, *Characterization of proton conducting CsHSO₄-CsH₂PO₄ ionic glasses prepared by the melt-quenching method*. Solid State Ionics, 2010. **181**(3-4): p. 190-192.
39. Oh, S.Y., T. Yoshida, G. Kawamura, H. Muto, M. Sakai, and A. Matsuda, *Composite electrolytes composed of Cs-substituted phosphotungstic acid and sulfonated poly(ether-ether ketone) for fuel cell systems*. Materials Science and Engineering B-Advanced Functional Solid-State Materials, 2010. **173**(1-3): p. 260-266.
40. Pawlaczyk, C., A. Pawlowski, M. Polomska, K. Pogorzelec-Glaser, B. Hilczer, A. Pietraszko, E. Markiewicz, P. Lawniczak, and L. Szczesniak, *Anhydrous proton conductors for use as solid electrolytes*. Phase Transitions, 2010. **83**(10-11): p. 854-867.
41. Xie, Q., Y.F. Li, J. Hu, X.J. Chen, and H.B. Li, *A CsH₂PO₄-based composite electrolyte membrane for intermediate temperature fuel cells (vol 489, pg 98, 2015)*. Journal of Membrane Science, 2015. **492**: p. 630-630.
42. Barron, O., H.N. Su, V. Linkov, B.G. Pollet, and S. Pasupathi, *CsHSO₄ as proton conductor for high-temperature polymer electrolyte membrane fuel cells*. Journal of Applied Electrochemistry, 2014. **44**(9): p. 1037-1045.
43. Guo, X.H., K.Q. Du, Y.X. Huang, H. Ge, Q.Z. Guo, Y. Wang, and F.H. Wang, *Application of a composite electrolyte in a solid-acid fuel cell system: A micro-arc oxidation alumina support filled with CsH₂PO₄*. International Journal of Hydrogen Energy, 2013. **38**(36): p. 16387-16393.
44. Timurkutluk, B., C. Timurkutluk, M.D. Mat, and Y. Kaplan, *A review on cell/stack designs for high performance solid oxide fuel cells*. Renewable & Sustainable Energy Reviews, 2016. **56**: p. 1101-1121.
45. Shaikh, S.P.S., A. Muchtar, and M.R. Somalu, *A review on the selection of anode materials for solid-oxide fuel cells*. Renewable & Sustainable Energy Reviews, 2015. **51**: p. 1-8.
46. Mahato, N., A. Banerjee, A. Gupta, S. Omar, and K. Balani, *Progress in material selection for solid oxide fuel cell technology: A review*. Progress in Materials Science, 2015. **72**: p. 141-337.

47. Yashima, M., *Invited Review: Some recent developments in the atomic-scale characterization of structural and transport properties of ceria-based catalysts and ionic conductors*. *Catalysis Today*, 2015. **253**: p. 3-19.
48. Wachsman, E.D. and K.T. Lee, *Lowering the Temperature of Solid Oxide Fuel Cells*. *Science*, 2011. **334**(6058): p. 935-939.
49. Zhu, L., R. Ran, M. Tadé, W. Wang, and Z. Shao, *Perovskite materials in energy storage and conversion*. *Asia-Pacific Journal of Chemical Engineering*, 2016. **11**(3): p. 338-369.
50. D'Epifanio, A., E. Fabbri, E. Di Bartolomeo, S. Licoccia, and E. Traversa, *BaZr(x)Y(1-x)O(3-delta) and BaCe(1-x-z)Zr(x)Y(z)O(3-delta) Proton Conductors For Intermediate Temperature Solid Oxide Fuel Cells (IT-SOFCs)*. *Solid Oxide Fuel Cells 10 (Sofc-X)*, Pts 1 and 2, 2007. **7**(1): p. 2337-2342.
51. D'Epifanio, A., E. Fabbri, E. Di Bartolomeo, S. Licoccia, and E. Traversa, *Design of BaZr_{0.8}Y_{0.2}O_{3-delta} protonic conductor to improve the electrochemical performance in intermediate temperature solid oxide fuel cells (IT-SOFCs)*. *Fuel Cells*, 2008. **8**(1): p. 69-76.
52. Zhu, Z.W., B.T. Liu, J.X. Shen, Y.X. Lou, and Y.X. Ji, *La₂Ce₂O₇: A promising proton ceramic conductor in hydrogen economy*. *Journal of Alloys and Compounds*, 2016. **659**: p. 232-239.
53. Kulkarni, A. and S. Giddey, *Materials issues and recent developments in molten carbonate fuel cells*. *Journal of Solid State Electrochemistry*, 2012. **16**(10): p. 3123-3146.
54. Cao, D.X., Y. Sun, and G.L. Wang, *Direct carbon fuel cell: Fundamentals and recent developments*. *Journal of Power Sources*, 2007. **167**(2): p. 250-257.
55. Rady, A.C., S. Giddey, S.P.S. Badwal, B.P. Ladewig, and S. Bhattacharya, *Review of Fuels for Direct Carbon Fuel Cells*. *Energy & Fuels*, 2012. **26**(3): p. 1471-1488.
56. Desclaux, P., M. Rzepka, U. Stimming, and R. Hempelmann, *Actual State of Technology in Direct Carbon Fuel Cells*. *Zeitschrift Fur Physikalische Chemie-International Journal of Research in Physical Chemistry & Chemical Physics*, 2013. **227**(5): p. 627-649.
57. Wellendorff, J., T.L. Silbaugh, D. Garcia-Pintos, J.K. Nørskov, T. Bligaard, F. Studt, and C.T. Campbell, *A benchmark database for adsorption bond energies to transition metal surfaces and comparison to selected DFT functionals*. *Surface Science*, 2015. **640**: p. 36-44.
58. Nilsson, A., L.G.M. Pettersson, B. Hammer, T. Bligaard, C.H. Christensen, and J.K. Nørskov, *The electronic structure effect in heterogeneous catalysis*. *Catalysis Letters*, 2005. **100**(3-4): p. 111-114.
59. Nørskov, J.K., J. Rossmeisl, A. Logadottir, L. Lindqvist, J.R. Kitchin, T. Bligaard, and H. Jonsson, *Origin of the overpotential for oxygen reduction at a fuel-cell cathode*. *The Journal of Physical Chemistry B*, 2004. **108**(46): p. 17886-17892.
60. Karlberg, G.S., T.F. Jaramillo, E. Skulason, J. Rossmeisl, T. Bligaard, and J.K. Nørskov, *Cyclic voltammograms for H on Pt (111) and Pt (100) from first principles*. *Physical review letters*, 2007. **99**(12): p. 126101.
61. Casalongue, H.S., S. Kaya, V. Viswanathan, D.J. Miller, D. Friebel, H.A. Hansen, J.K. Nørskov, A. Nilsson, and H. Ogasawara, *Direct observation of the oxygenated species during oxygen reduction on a platinum fuel cell cathode*. *Nature communications*, 2013. **4**.
62. Christensen, C.H. and J.K. Nørskov, *A molecular view of heterogeneous catalysis*. *The Journal of chemical physics*, 2008. **128**(18): p. 182503.

63. Rossmeisl, J. and W.G. Bessler, *Trends in catalytic activity for SOFC anode materials*. Solid State Ionics, 2008. **178**(31): p. 1694-1700.
64. Conner Jr, W.C. and J.L. Falconer, *Spillover in heterogeneous catalysis*. Chemical reviews, 1995. **95**(3): p. 759-788.
65. Reiss, H., *The Fermi level and the redox potential*. The Journal of Physical Chemistry, 1985. **89**(18): p. 3783-3791.
66. Elahi, A. and D.J. Caruana, *Plasma electrochemistry: voltammetry in a flame plasma electrolyte*. Physical Chemistry Chemical Physics, 2013. **15**(4): p. 1108-1114.
67. Ghoroghchian, J., F. Sarfarazi, T. Dibble, J. Cassidy, J.J. Smith, A. Russell, G. Dunmore, M. Fleischmann, and S. Pons, *Electrochemistry in the Gas-Phase - Use of Ultramicroelectrodes for the Analysis of Electroactive Species in Gas-Mixtures*. Analytical Chemistry, 1986. **58**(11): p. 2278-2282.
68. Toghill, K.E., M.A. Mendez, and P. Voyame, *Electrochemistry in supercritical fluids: A mini review*. Electrochemistry Communications, 2014. **44**: p. 27-30.
69. Bagotskiĭ, V.S., *Fundamentals of electrochemistry*. 2nd ed. The Electrochemical Society series 2006, Hoboken, N.J.: Wiley-Interscience. xxviii, 722 p.
70. Kharton, V.V., *Solid state electrochemistry* 2009, Weinheim ; Chichester: Wiley-VCH. v. <2>.
71. Bard, A.J. and L.R. Faulkner, *Electrochemical methods : fundamentals and applications*. 2nd ed 2001, New York: Wiley. xxi, 833 p.
72. Larminie, J. and A. Dicks, *Fuel cell systems explained*. 2nd ed 2003, Chichester, West Sussex: J. Wiley. xxii, 406 p.
73. Huang, K. and J.B. Goodenough, *2 - Thermodynamics of the solid oxide fuel cell (SOFC)*, in *Solid Oxide Fuel Cell Technology* 2009, Woodhead Publishing. p. 10-22.
74. Zhang, J., *PEM fuel cell electrocatalysts and catalyst layers : fundamentals and applications* 2008, London: Springer. xxi, 1137 p.
75. Kreuer, K.D., A. Rabenau, and W. Weppner, *Vehicle Mechanism, a New Model for the Interpretation of the Conductivity of Fast Proton Conductors*. Angewandte Chemie-International Edition in English, 1982. **21**(3): p. 208-209.
76. Kreuer, K.D., *Proton conductivity: Materials and applications*. Chemistry of Materials, 1996. **8**(3): p. 610-641.
77. Rumberger, B., M. Bennett, J.Y. Zhang, J.A. Dura, and N.E. Israeloff, *Communication: Nanoscale ion fluctuations in Nafion polymer electrolyte*. Journal of Chemical Physics, 2014. **141**(7).
78. Aleksandrova, E., R. Hiesgen, K.A. Friedrich, and E. Roduner, *Electrochemical atomic force microscopy study of proton conductivity in a Nafion membrane*. Physical Chemistry Chemical Physics, 2007. **9**(21): p. 2735-2743.
79. Vilčiauskas, L., M.E. Tuckerman, G. Bester, S.J. Paddison, and K.D. Kreuer, *The mechanism of proton conduction in phosphoric acid*. Nature Chemistry, 2012. **4**(6): p. 461-466.
80. Vilčiauskas, L., S.J. Paddison, and K.D. Kreuer, *Ab Initio Modeling of Proton Transfer in Phosphoric Acid Clusters*. Journal of Physical Chemistry A, 2009. **113**(32): p. 9193-9201.
81. Kidena, K., T. Ohkubo, N. Takimoto, and A. Ohira, *PFM-NMR approach to determining the water transport mechanism in polymer electrolyte membranes conditioned at different temperatures*. European Polymer Journal, 2010. **46**(3): p. 450-455.

82. Luduena, G.A., T.D. Kuhne, and D. Sebastiani, *Mixed Grotthuss and Vehicle Transport Mechanism in Proton Conducting Polymers from Ab initio Molecular Dynamics Simulations*. Chemistry of Materials, 2011. **23**(6): p. 1424-1429.
83. Walden, P., *internal friction and its connection with conductivity*. zeitschrift für physikalische chemie stöchiometrie und verwandtschaftslehre 1906. **55**: p. 207-249.
84. Mendolia, M.S. and G.C. Farrington, *Ionic Mobility in Macromolecular Electrolytes - the Failure of Walden Rule*. Chemistry of Materials, 1993. **5**(2): p. 174-181.
85. Kerres, J., A. Ullrich, T. Haring, M. Baldauf, U. Gebhardt, and W. Preidel, *Preparation, characterization and fuel cell application of new acid-base blend membranes*. Journal of New Materials for Electrochemical Systems, 2000. **3**(3): p. 229-239.
86. Hwang, K., J.H. Kim, S.Y. Kim, and H. Byun, *Preparation of Polybenzimidazole-Based Membranes and Their Potential Applications in the Fuel Cell System*. Energies, 2014. **7**(3): p. 1721-1732.
87. Mack, F., S. Heissler, R. Laukenmann, and R. Zeis, *Phosphoric acid distribution and its impact on the performance of polybenzimidazole membranes*. Journal of Power Sources, 2014. **270**: p. 627-633.
88. Zhang, C.Z., L. Zhang, W.J. Zhou, Y.Y. Wang, and S.H. Chan, *Investigation of water transport and its effect on performance of high-temperature PEM fuel cells*. Electrochimica Acta, 2014. **149**: p. 271-277.
89. Pahari, S., C.K. Choudhury, P.R. Pandey, M. More, A. Venkatnathan, and S. Roy, *Molecular Dynamics Simulation of Phosphoric Acid Doped Monomer of Polybenzimidazole: A Potential Component Polymer Electrolyte Membrane of Fuel Cell*. Journal of Physical Chemistry B, 2012. **116**(24): p. 7357-7366.
90. Ebnesajjad, S., *Fluoroplastics : the definitive user's guide and databook*. PDL handbook series2000, Norwich, NY: Plastics Design Library.
91. Dlubek, G., M.A. Alam, K. Saarinen, J. Stejny, and H.M. Fretwell, *Relations between hole volume and macroscopic volume in various polymers*. Acta Physica Polonica A, 1999. **95**(4): p. 521-526.
92. <http://www.sigmaaldrich.com/technical-documents/articles/materials-science/perfluorosulfonic-acid-membranes.html>.
93. Arcella, V., C. Troglia, and A. Ghielmi, *Hyflon ion membranes for fuel cells*. Industrial & Engineering Chemistry Research, 2005. **44**(20): p. 7646-7651.
94. Teng, H.X., *Overview of the Development of the Fluoropolymer Industry*. Applied Sciences-Basel, 2012. **2**(2): p. 496-512.
95. Emery, M., M. Frey, M. Guerra, G. Haugen, K. Hintzer, K.H. Lochhaas, P. Pham, D. Pierpont, M. Schaberg, A. Thaler, M. Yandrasits, and S. Hamrock, *The Development of New Membranes for Proton Exchange Membrane Fuel Cells*. Polymer Electrolyte Fuel Cells 14, 2007. **11**(1): p. 3-14.
96. Curtin, D.E., R.D. Lousenberg, T.J. Henry, P.C. Tangeman, and M.E. Tisack, *Advanced materials for improved PEMFC performance and life*. Journal of Power Sources, 2004. **131**(1-2): p. 41-48.
97. Park, C.H., C.H. Lee, M.D. Guiver, and Y.M. Lee, *Sulfonated hydrocarbon membranes for medium-temperature and low-humidity proton exchange membrane fuel cells (PEMFCs)*. Progress in Polymer Science, 2011. **36**(11): p. 1443-1498.

98. Serpico, J.M., S.G. Ehrenberg, J.J. Fontanella, X. Jiao, D. Perahia, K.A. McGrady, E.H. Sanders, G.E. Kellogg, and G.E. Wnek, *Transport and structural studies of sulfonated styrene-ethylene copolymer membranes*. *Macromolecules*, 2002. **35**(15): p. 5916-5921.
99. Kim, J., B. Kim, and B. Jung, *Proton conductivities and methanol permeabilities of membranes made from partially sulfonated polystyrene-block-poly(ethylene-ran-butylene)-block-polystyrene copolymers*. *Journal of Membrane Science*, 2002. **207**(1): p. 129-137.
100. Genies, C., R. Mercier, B. Sillion, N. Cornet, G. Gebel, and M. Pineri, *Soluble sulfonated naphthalenic polyimides as materials for proton exchange membranes*. *Polymer*, 2001. **42**(2): p. 359-373.
101. Kobayashi, T., M. Rikukawa, K. Sanui, and N. Ogata, *Proton-conducting polymers derived from poly(ether-etherketone) and poly(4-phenoxybenzoyl-1,4-phenylene)*. *Solid State Ionics*, 1998. **106**(3-4): p. 219-225.
102. Hickner, M.A., H. Ghassemi, Y.S. Kim, B.R. Einsla, and J.E. McGrath, *Alternative polymer systems for proton exchange membranes (PEMs)*. *Chemical Reviews*, 2004. **104**(10): p. 4587-4611.
103. Guo, Q.H., P.N. Pintauro, H. Tang, and S. O'Connor, *Sulfonated and crosslinked polyphosphazene-based proton-exchange membranes*. *Journal of Membrane Science*, 1999. **154**(2): p. 175-181.
104. Wycisk, R., P.N. Pintauro, W. Wang, and S. O'Connor, *Polyphosphazene membranes .I. Solid-state photocrosslinking of poly[(4-ethylphenoxy)(phenoxy)phosphazene]*. *Journal of Applied Polymer Science*, 1996. **59**(10): p. 1607-1617.
105. Gao, X.M., Y.H. Liu, and J.L. Li, *Review on Modification of Sulfonated Poly (-ether-ether-ketone) Membranes Used as Proton Exchange Membranes*. *Materials Science-Medziagotyra*, 2015. **21**(4): p. 574-582.
106. Jaafar, J., A.F. Ismail, and A. Mustafa, *Physicochemical study of poly(ether ether ketone) electrolyte membranes sulfonated with mixtures of fuming sulfuric acid and sulfuric acid for direct methanol fuel cell application*. *Materials Science and Engineering a-Structural Materials Properties Microstructure and Processing*, 2007. **460**: p. 475-484.
107. Ueda, M., H. Toyota, T. Ouchi, J.I. Sugiyama, K. Yonetake, T. Masuko, and T. Teramoto, *Synthesis and Characterization of Aromatic Poly(Ether Sulfone)S Containing Pendant Sodium-Sulfonate Groups*. *Journal of Polymer Science Part a-Polymer Chemistry*, 1993. **31**(4): p. 853-858.
108. Wang, F., T.L. Chen, and J.P. Xu, *Sodium sulfonate-functionalized poly(ether ether ketone)s*. *Macromolecular Chemistry and Physics*, 1998. **199**(7): p. 1421-1426.
109. Wang, F., M. Hickner, Q. Ji, W. Harrison, J. Mecham, T.A. Zawodzinski, and J.E. McGrath, *Synthesis of highly sulfonated poly(arylene ether sulfone) random (statistical) copolymers via direct polymerization*. *Macromolecular Symposia*, 2001. **175**: p. 387-395.
110. Wang, F., M. Hickner, Y.S. Kim, T.A. Zawodzinski, and J.E. McGrath, *Direct polymerization of sulfonated poly(arylene ether sulfone) random (statistical) copolymers: candidates for new proton exchange membranes*. *Journal of Membrane Science*, 2002. **197**(1-2): p. 231-242.
111. Vallejo, E., G. Pourcelly, C. Gavach, R. Mercier, and M. Pineri, *Sulfonated polyimides as proton conductor exchange membranes. Physicochemical properties and separation H⁺/Mz⁺ by electrodialysis comparison with a perfluorosulfonic membrane*. *Journal of Membrane Science*, 1999. **160**(1): p. 127-137.

112. Cornet, N., O. Diat, G. Gebel, F. Jousse, D. Marsacq, R. Mercier, and M. Pineri, *Sulfonated polyimide membranes: a new type of ion-conducting membrane for electrochemical applications*. Journal of New Materials for Electrochemical Systems, 2000. **3**(1): p. 33-42.
113. Detallante, V., D. Langevin, C. Chappey, M. Metayer, R. Mercier, and M. Pineri, *Kinetics of water vapor sorption in sulfonated polyimide membranes*. Desalination, 2002. **148**(1-3): p. 333-339.
114. Shi, H.F., Y. Zhao, X. Dong, Y. Zhou, and D.J. Wang, *Frustrated crystallisation and hierarchical self-assembly behaviour of comb-like polymers*. Chemical Society Reviews, 2013. **42**(5): p. 2075-2099.
115. Ben youcef, H., L. Gubler, S.A. Gursel, D. Henkensmeier, A. Wokaun, and G.G. Scherer, *Novel ETFE based radiation grafted poly(styrene sulfonic acid-co-methacrylonitrile) proton conducting membranes with increased stability*. Electrochemistry Communications, 2009. **11**(5): p. 941-944.
116. Ben youcef, H., L. Gubler, T. Yamaki, S. Sawada, S.A. Gursel, A. Wokaun, and G.G. Scherer, *Cross-Linker Effect in ETFE-Based Radiation-Grafted Proton-Conducting Membranes*. Journal of The Electrochemical Society, 2009. **156**(4): p. B532-B539.
117. Ben youcef, H., S.A. Gursel, A. Buisson, L. Gubler, A. Wokaun, and G.G. Scherer, *Influence of Radiation-Induced Grafting Process on Mechanical Properties of ETFE-Based Membranes for Fuel Cells*. Fuel Cells, 2010. **10**(3): p. 401-410.
118. Ben Youcef, H., S.A. Gursel, A. Wokaun, and G.G. Scherer, *The influence of crosslinker on the properties of radiation-grafted films and membranes based on ETFE*. Journal of Membrane Science, 2008. **311**(1-2): p. 208-215.
119. Dogan, H.D.C. and S.A. Gursel, *Preparation and Characterisation of Novel Composites Based on a Radiation Grafted Membrane for Fuel Cells*. Fuel Cells, 2011. **11**(3): p. 361-371.
120. Farquet, P., C. Padeste, M. Borner, H. Ben Youcef, S.A. Gursel, G.G. Scherer, H.H. Solaka, V. Sailec, and A. Wokaun, *Microstructured proton-conducting membranes by synchrotron-radiation-induced grafting*. Journal of Membrane Science, 2008. **325**(2): p. 658-664.
121. Farquet, P., C. Padeste, H.H. Solak, S.A. Gursel, G.G. Scherer, and A. Wokaun, *Extreme UV radiation grafting of glycidyl methacrylate nanostructures onto fluoropolymer foils by RAFT-mediated polymerization*. Macromolecules, 2008. **41**(17): p. 6309-6316.
122. Gubler, L., S.A. Gursel, and G.G. Scherer, *Radiation grafted membranes for polymer electrolyte fuel cells*. Fuel Cells, 2005. **5**(3): p. 317-335.
123. Gubler, L., N. Prost, S.A. Gursel, and G.G. Scherer, *Proton exchange membranes prepared by radiation grafting of styrene/divinylbenzene onto poly(ethylene-alt-tetrafluoroethylene) for low temperature fuel cells*. Solid State Ionics, 2005. **176**(39-40): p. 2849-2860.
124. Gubler, L., H.B. Youcef, S.A. Gursel, A. Wokaun, and G.G. Scherer, *Cross-linker effect in ETFE-based radiation-grafted proton-conducting membranes - I. Properties and fuel cell performance characteristics*. Journal of The Electrochemical Society, 2008. **155**(9): p. B921-B928.
125. Gubler, L., H.B. Youcef, S.A. Gursel, A. Wokaun, and G.G. Scherer, *Cross-linker effect in ETFE-Based radiation-grafted proton-conducting membranes (vol 155, pg B921, 2008)*. Journal of The Electrochemical Society, 2008. **155**(10): p. S7-S7.

126. Gursel, S.A., H. Ben Youcef, A. Wokaun, and G.G. Scherer, *Influence of reaction parameters on grafting of styrene into poly(ethylene-alt-tetrafluoroethylene) films*. Nuclear Instruments & Methods in Physics Research Section B-Beam Interactions with Materials and Atoms, 2007. **265**(1): p. 198-203.
127. Gursel, S.A., L. Gubler, B. Gupta, and G.G. Scherer, *Radiation Grafted Membranes*. Fuel Cells I, 2008. **215**: p. 157-217.
128. Gursel, S.A., C. Padeste, H.H. Solak, and G.G. Scherer, *Microstructured polymer films by X-ray lithographic exposure and grafting*. Nuclear Instruments & Methods in Physics Research Section B-Beam Interactions with Materials and Atoms, 2005. **236**: p. 449-455.
129. Gursel, S.A., J. Schneider, H. Ben Youcef, A. Wokaun, and G.G. Scherer, *Thermal properties of proton-conducting radiation-grafted membranes*. Journal of Applied Polymer Science, 2008. **108**(6): p. 3577-3585.
130. Gursel, S.A., Z. Yang, B. Choudhury, M.G. Roelofs, and G.G. Scherer, *Radiation-grafted membranes using a trifluorostyrene derivative*. Journal of the Electrochemical Society, 2006. **153**(10): p. A1964-A1970.
131. Mortensen, K., U. Gasser, S.A. Gursel, and G.G. Scherer, *Structural characterization of radiation-grafted block copolymer films, using SANS technique*. Journal of Polymer Science Part B-Polymer Physics, 2008. **46**(16): p. 1660-1668.
132. Sanli, L.I. and S.A. Gursel, *Synthesis and Characterization of Novel Graft Copolymers by Radiation-Induced Grafting*. Journal of Applied Polymer Science, 2011. **120**(4): p. 2313-2323.
133. Nasef, M.M., E. Shamsaei, H. Saidi, A. Ahmad, and K.Z.M. Dahlan, *Preparation and Characterization of Phosphoric Acid Composite Membrane by Radiation Induced Grafting of 4-Vinylpyridine onto Poly(ethylene-co-tetrafluoroethylene) Followed by Phosphoric Acid Doping*. Journal of Applied Polymer Science, 2013. **128**(1): p. 549-557.
134. Jetsrisuparb, K., H. Ben youcef, A. Wokaun, and L. Gubler, *Radiation grafted membranes for fuel cells containing styrene sulfonic acid and nitrile comonomers*. Journal of Membrane Science, 2014. **450**: p. 28-37.
135. Gubler, L., M. Slaski, A. Wokaun, and G.G. Scherer, *Advanced monomer combinations for radiation grafted fuel cell membranes*. Electrochemistry Communications, 2006. **8**(8): p. 1215-1219.
136. Varcoe, J.R., R.C.T. Slade, E.L.H. Yee, S.D. Poynton, D.J. Driscoll, and D.C. Apperley, *Poly(ethylene-co-tetrafluoroethylene)-derived radiation-grafted anion-exchange membrane with properties specifically tailored for application in metal-cation-free alkaline polymer electrolyte fuel cells*. Chemistry of Materials, 2007. **19**(10): p. 2686-2693.
137. Poynton, S.D., R.C.T. Slade, T.J. Omasta, W.E. Mustain, R. Escudero-Cid, P. Ocon, and J.R. Varcoe, *Preparation of radiation-grafted powders for use as anion exchange ionomers in alkaline polymer electrolyte fuel cells*. Journal of Materials Chemistry A, 2014. **2**(14): p. 5124-5130.
138. Danks, T.N., R.C.T. Slade, and J.R. Varcoe, *Comparison of PVDF- and FEP-based radiation-grafted alkaline anion-exchange membranes for use in low temperature portable DMFCs*. Journal of Materials Chemistry, 2002. **12**(12): p. 3371-3373.
139. Jacob Spendelow, J.M., *Fuel Cell System Cost*. DOE Fuel Cell Technologies Office Record, 2014.

140. Nasef, M.M., *Radiation-Grafted Membranes for Polymer Electrolyte Fuel Cells: Current Trends and Future Directions*. Chemical reviews, 2014. **114**(24): p. 12278-12329.
141. Nasef, M.M., H. Saidi, and K.M. Dahlan, *Comparative investigations of radiation-grafted proton-exchange membranes prepared using single-step and conventional two-step radiation-induced grafting methods*. Polymer International, 2011. **60**(2): p. 186-193.
142. Kang, G.D. and Y.M. Cao, *Application and modification of poly(vinylidene fluoride) (PVDF) membranes - A review*. Journal of Membrane Science, 2014. **463**: p. 145-165.
143. Liu, F., N.A. Hashim, Y.T. Liu, M.R.M. Abed, and K. Li, *Progress in the production and modification of PVDF membranes*. Journal of Membrane Science, 2011. **375**(1-2): p. 1-27.
144. Li, M.Y., I. Katsouras, C. Piliago, G. Glasser, I. Lieberwirth, P.W.M. Blom, and D.M. de Leeuw, *Controlling the microstructure of poly(vinylidene-fluoride) (PVDF) thin films for microelectronics*. Journal of Materials Chemistry C, 2013. **1**(46): p. 7695-7702.
145. Lehtinen, T., G. Sundholm, S. Holmberg, F. Sundholm, P. Bjornbom, and M. Bursell, *Electrochemical characterization of PVDF-based proton conducting membranes for fuel cells*. Electrochimica Acta, 1998. **43**(12-13): p. 1881-1890.
146. Flint, S.D. and R.C.T. Slade, *Investigation of radiation-grafted PVDF-g-polystyrene-sulfonic-acid ion exchange membranes for use in hydrogen oxygen fuel cells*. Solid State Ionics, 1997. **97**(1-4): p. 299-307.
147. Li, L.F., B. Deng, Y.L. Ji, Y. Yu, L.D. Xie, J.Y. Li, and X.F. Lu, *A novel approach to prepare proton exchange membranes from fluoropolymer powder by pre-irradiation induced graft polymerization*. Journal of Membrane Science, 2010. **346**(1): p. 113-120.
148. Kim, Y.W., D.K. Lee, K.J. Lee, and J.H. Kim, *Single-step synthesis of proton conducting poly(vinylidene fluoride) (PVDF) graft copolymer electrolytes*. European Polymer Journal, 2008. **44**(3): p. 932-939.
149. Su, Y.H., Y.L. Liu, D.M. Wang, J.Y. Lai, Y.M. Sun, S.D. Chyou, and W.T. Lee, *The effect of side chain architectures on the properties and proton conductivities of poly(styrene sulfonic acid) graft poly(vinylidene fluoride) copolymer membranes for direct methanol fuel cells*. Journal of Membrane Science, 2010. **349**(1-2): p. 244-250.
150. Kim, S.K., J.H. Ryu, H.D. Kwen, C.H. Chang, and S.H. Cho, *Convenient Preparation of Ion-Exchange PVdF Membranes by a Radiation-Induced Graft Polymerization for a Battery Separator*. Polymer-Korea, 2010. **34**(2): p. 126-132.
151. Nasef, M.M., H. Saidi, and K.Z.M. Dahlan, *Single-step radiation induced grafting for preparation of proton exchange membranes for fuel cell*. Journal of Membrane Science, 2009. **339**(1-2): p. 115-119.
152. Nasef, M.M., H. Saidi, and K.Z.M. Dahlan, *Acid-Synergized Grafting of Sodium Styrene Sulfonate onto Electron Beam Irradiated-Poly(vinylidene fluoride) Films for Preparation of Fuel Cell Membrane*. Journal of Applied Polymer Science, 2010. **118**(5): p. 2801-2809.
153. M. G. Roelofs, Z. Yang, S. Alkan Gürsel, G. G. Scherer 'Process to Prepare Stable Trifluorostyrene Containing Compounds Grafted to Base Polymers using an Alcohol/Water Mixture' WO2006102672 (28-09-2006).
154. Okamura, H., Y. Takatori, M. Tsunooka, and M. Shirai, *Synthesis of random and block copolymers of styrene and styrenesulfonic acid with low polydispersity using nitroxide-mediated living radical polymerization technique*. Polymer, 2002. **43**(11): p. 3155-3162.

155. Hester, J.F., P. Banerjee, Y.Y. Won, A. Akthakul, M.H. Acar, and A.M. Mayes, *ATRP of amphiphilic graft copolymers based on PVDF and their use as membrane additives*. *Macromolecules*, 2002. **35**(20): p. 7652-7661.
156. Gupta, B., N. Grover, and H. Singh, *Radiation Grafting of Acrylic Acid onto Poly(ethylene terephthalate) Fabric*. *Journal of Applied Polymer Science*, 2009. **112**(3): p. 1199-1208.
157. Lappan, U., U. Geissler, and S. Uhlmann, *Radiation-induced grafting of styrene into radiation-modified fluoropolymer films*. *Nuclear Instruments & Methods in Physics Research Section B-Beam Interactions with Materials and Atoms*, 2005. **236**: p. 413-419.
158. Arunbabu, D., Z. Sanga, K.M. Seenimeera, and T. Jana, *Emulsion copolymerization of styrene and sodium styrene sulfonate: kinetics, monomer reactivity ratios and copolymer properties*. *Polymer International*, 2009. **58**(1): p. 88-96.
159. Zhang, W.J., R. Wycisk, D.L. Kish, and P.N. Pintauro, *Pre-Stretched Low Equivalent Weight PFSA Membranes with Improved Fuel Cell Performance*. *Journal of the Electrochemical Society*, 2014. **161**(6): p. F770-F777.
160. Jiang, D.D., Q. Yao, M.A. McKinney, and C.A. Wilkie, *TGA/FTIR studies on the thermal degradation of some polymeric sulfonic and phosphonic acids and their sodium salts*. *Polymer Degradation and Stability*, 1999. **63**(3): p. 423-434.
161. Baschuk, J.J. and X.G. Li, *Carbon monoxide poisoning of proton exchange membrane fuel cells*. *International Journal of Energy Research*, 2001. **25**(8): p. 695-713.
162. Li, H., Y.H. Tang, Z.W. Wang, Z. Shi, S.H. Wu, D.T. Song, J.L. Zhang, K. Fatih, J.J. Zhang, H.J. Wang, Z.S. Liu, R. Abouatallah, and A. Mazza, *A review of water flooding issues in the proton exchange membrane fuel cell*. *Journal of Power Sources*, 2008. **178**(1): p. 103-117.
163. Matos, B.R., M.A. Dresch, E.I. Santiago, L.P.R. Moraes, D.J. Carastan, J. Schoenmaker, I.A. Velasco-Davalos, A. Ruediger, A.C. Tavares, and F.C. Fonseca, *Nafion membranes annealed at high temperature and controlled humidity: structure, conductivity, and fuel cell performance*. *Electrochimica Acta*, 2016. **196**: p. 110-117.
164. Hink, S., N. Wagner, W.G. Bessler, and E. Roduner, *Impedance Spectroscopic Investigation of Proton Conductivity in Nafion Using Transient Electrochemical Atomic Force Microscopy (AFM)*. *Membranes*, 2012. **2**(2).
165. Paidar, M., J. Malis, K. Bouzek, and J. Zitka, *Behavior of Nafion membrane at elevated temperature and pressure*. *Desalination and Water Treatment*, 2010. **14**(1-3): p. 106-111.
166. Oono, Y., A. Sounai, and M. Hori, *Influence of the phosphoric acid-doping level in a polybenzimidazole membrane on the cell performance of high-temperature proton exchange membrane fuel cells*. *Journal of Power Sources*, 2009. **189**(2): p. 943-949.
167. Kawahara, M., M. Rikukawa, and K. Sanui, *Relationship between absorbed water and proton conductivity in sulfopropylated poly(benzimidazole)*. *Polymers for Advanced Technologies*, 2000. **11**(8-12): p. 544-547.
168. Pu, H.T. and Q.Z. Liu, *Methanol permeability and proton conductivity of polybenzimidazole and sulfonated polybenzimidazole*. *Polymer International*, 2004. **53**(10): p. 1512-1516.
169. Papadimitriou, K.D., A.K. Andreopoulou, and J.K. Kallitsis, *Phosphonated Fully Aromatic Polyethers for PEMFCs Applications*. *Journal of Polymer Science Part A-Polymer Chemistry*, 2010. **48**(13): p. 2817-2827.

170. Thomas, O.D., T.J. Peckham, U. Thanganathan, Y.S. Yang, and S. Holdcroft, *Sulfonated Polybenzimidazoles: Proton Conduction and Acid-Base Crosslinking*. Journal of Polymer Science Part a-Polymer Chemistry, 2010. **48**(16): p. 3640-3650.
171. Takrori, F., *Grafting of nitrogen containing monomers onto poly(ethylene-alt-tetrafluoroethylene) films by bulk polymerization for proton exchange membranes*. Journal of Radioanalytical and Nuclear Chemistry, 2016. **308**(3): p. 1089-1094.
172. Sithambaranathan, P., M.M. Nasef, and A. Ahmad, *Kinetic behaviour of graft copolymerisation of nitrogenous heterocyclic monomer onto EB-irradiated ETFE films*. Journal of Radioanalytical and Nuclear Chemistry, 2015. **304**(3): p. 1225-1234.
173. Schmidt, C. and G. Schmidt-Naake, *Proton conducting membranes obtained by doping radiation-grafted basic membrane matrices with phosphoric add*. Macromolecular Materials and Engineering, 2007. **292**(10-11): p. 1164-1175.
174. Sithambaranathan, P., M.M. Nasef, A. Ahmad, and A. Ripin, *Crosslinked composite membrane by radiation grafting of 4-vinylpyridine/triallyl-cyanurate mixtures onto poly(ethylene-co-tetrafluoroethylene) and phosphoric acid doping*. International Journal of Hydrogen Energy.
175. Chen, J.H., M. Asano, T. Yamaki, and M. Yoshida, *Effect of crosslinkers on the preparation and properties of ETFE-based radiation-grafted polymer electrolyte membranes*. Journal of Applied Polymer Science, 2006. **100**(6): p. 4565-4574.
176. Si, Y.F. and Z.G. Guo, *Superhydrophobic nanocoatings: from materials to fabrications and to applications*. Nanoscale, 2015. **7**(14): p. 5922-5946.
177. Zeis, R., *Materials and characterization techniques for high-temperature polymer electrolyte membrane fuel cells*. Beilstein Journal of Nanotechnology, 2015. **6**: p. 68-83.

The End